

1 **Trends in secondary inorganic aerosol pollution in China and its responses to**
2 **emission controls of precursors in wintertime**

3 Fanlei Meng^{1#}, Yibo Zhang^{2#}, Jiahui Kang¹, Mathew R. Heal³, Stefan Reis^{4,3,5}, Mengru
4 Wang⁶, Lei Liu⁷, Kai Wang¹, Shaocai Yu^{2*}, Pengfei Li⁸, Jing Wei⁹, Yong Hou¹, Ying
5 Zhang¹, Xuejun Liu¹, Zhenling Cui¹, Wen Xu^{1*}, Fusuo Zhang¹

6
7 ¹College of Resource and Environmental Sciences; National Academy of Agriculture
8 Green Development; Key Laboratory of Plant-Soil Interactions of MOE, Beijing Key
9 Laboratory of Cropland Pollution Control and Remediation, China Agricultural
10 University, Beijing 100193, China.

11 ²Research Center for Air Pollution and Health, Key Laboratory of Environmental
12 Remediation and Ecological Health, Ministry of Education, College of Environment
13 and Resource Sciences, Zhejiang University, Hangzhou, Zhejiang 310058, P.R. China

14 ³School of Chemistry, The University of Edinburgh, David Brewster Road, Edinburgh
15 EH9 3FJ, United Kingdom

16 ⁴UK Centre for Ecology & Hydrology, Penicuik, EH26 0QB, United Kingdom.

17 ⁵University of Exeter Medical School, Knowledge Spa, Truro, TR1 3HD United
18 Kingdom.

19 ⁶Water Systems and Global Change Group, Wageningen University & Research, P.O.
20 Box 47, 6700 AA Wageningen, The Netherlands

21 ⁷College of Earth and Environmental Sciences, Lanzhou University, Lanzhou 730000,
22 China

23 ⁸College of Science and Technology, Hebei Agricultural University, Baoding, Hebei
24 071000, China

25 ⁹Department of Atmospheric and Oceanic Science, Earth System Science
26 Interdisciplinary Center, University of Maryland, College Park 20740, USA

27

28 *Corresponding authors

29 E-mail addresses: W. Xu (wenxu@cau.edu.cn); S C. Yu (shaocaiyu@zju.edu.cn)

30 # Contributed equally to this work.

31

32

33 **ABSTRACT:** The Chinese government recently proposed ammonia (NH₃) emissions
34 reductions (but without a specific national target) as a strategic option to mitigate PM_{2.5}
35 pollution. We combined a meta-analysis of nationwide measurements and air quality
36 modelling to identify efficiency gains by striking a balance between controlling NH₃
37 and acid gas (SO₂ and NO_x) emissions. We found that PM_{2.5} concentrations decreased
38 from 2000 to 2019, but annual mean PM_{2.5} concentrations still exceeded 35 μg m⁻³ at
39 74% of 1498 monitoring sites in 2015-2019. The concentration of PM_{2.5} and its
40 components were significantly higher (16%-195%) on hazy days than on non-hazy days.
41 Compared with mean values of other components, this difference was more significant
42 for the secondary inorganic ions SO₄²⁻, NO₃⁻, and NH₄⁺ (average increase 98%). While
43 sulfate concentrations significantly decreased over the time period, no significant
44 change was observed for nitrate and ammonium concentrations. Model simulations
45 indicate that the effectiveness of a 50% NH₃ emission reduction for controlling SIA
46 concentrations decreased from 2010 to 2017 in four megacity clusters of eastern China,
47 simulated for the month of January under fixed meteorological conditions (2010).
48 Although the effectiveness further declined in 2020 for simulations including the
49 natural experiment of substantial reductions in acid gas emissions during the COVID-
50 19 pandemic, the resulting reductions in SIA concentrations were on average 20.8%
51 lower than that in 2017. In addition, the reduction of SIA concentrations in 2017 was
52 greater for 50% acid gas reductions than for the 50% NH₃ emissions reduction. Our
53 findings indicate that persistent secondary inorganic aerosol pollution in China is
54 limited by acid gases emissions, while an additional control on NH₃ emissions would
55 become more important as reductions of SO₂ and NO_x emissions progress.

56

删除了: Secondary inorganic aerosols (SIA) were the dominant contributor to ambient PM_{2.5} concentrations.

59 **Keywords:** Air pollution, Particulate matter, Second inorganic aerosols, Anthropogenic
60 emission, Ammonia.

61

62 **1. Introduction**

63 Over the past two decades, China has experienced severe PM_{2.5} (particulate matter
64 with aerodynamic diameter $\leq 2.5 \mu\text{m}$) pollution (Huang et al., 2014; Wang et al., 2016),
65 leading to adverse impacts on human health (Liang et al., 2020) and the environment
66 (Yue et al., 2020). In 2019, elevated PM_{2.5} concentrations accounted for 46% of polluted
67 days in China and PM_{2.5} was officially identified as a key year-round air pollutant
68 (MEEP, 2019). Mitigation of PM_{2.5} pollution is therefore the most pressing current
69 challenge to improve China's air quality.

70 The Chinese government has put a major focus on particulate air pollution control
71 through a series of policies, regulations, and laws to prevent and control severe air
72 pollution. Before 2010, the Chinese government mainly focused on controlling SO₂
73 emissions via improvement of energy efficiency, with less attention paid to NO_x
74 abatement (CSC, 2007, 2011, 2016). For example, the 11th Five-Year Plan (FYP) (2006-
75 2010) set a binding goal of a 10% reduction for SO₂ emission (CSC, 2007). The 12th
76 FYP (2011-2015) added NO_x regulation and required 8% and 10% reductions for SO₂
77 and NO_x emissions, respectively (CSC, 2011) This was followed by further reductions
78 in SO₂ and NO_x emissions of 15% and 10%, respectively, in the 13th FYP (2016-2020)
79 (CSC, 2016). In response to the severe haze events of 2013, the Chinese State Council
80 promulgated the toughest-ever 'Atmospheric Pollution Prevention and Control Action
81 Plan' in September 2013, aiming to reduce ambient PM_{2.5} concentrations by 15-20% in
82 2017 relative to 2013 levels in metropolitan regions (CSC, 2013). As a result of the
83 implementation of stringent control measures, emissions reductions markedly

84 accelerated from 2013-2017, with decreases of 59% for SO₂, 21% for NO_x, and 33%
85 for primary PM_{2.5} (Zheng et al., 2018). Consequently, significant reductions in annual
86 mean PM_{2.5} concentrations were observed nationwide (Zhang et al., 2019; Yue et al.,
87 2020), in the range 28-40% in the metropolitan regions (CSC, 2018a). To continue its
88 efforts in tackling air pollution, China promulgated the Three-Year Action Plan (TYAP)
89 in 2018 for Winning the Blue-Sky Defense Battle (CSC, 2018b), which required a
90 further 15% reduction in NO_x emissions by 2020 compared to 2018 levels.

91 Despite a substantial reduction in PM_{2.5} concentrations in China, the proportion of
92 secondary aerosols during severe haze periods is increasing (An et al., 2019), and can
93 comprise up to 70% of PM_{2.5} concentrations (Huang et al., 2014). Secondary inorganic
94 aerosols (SIA, the sum of sulfate (SO₄²⁻), nitrate (NO₃⁻), and ammonium (NH₄⁺)) were
95 found to be of equal importance to secondary organic aerosols, with 40-50%
96 contributions to PM_{2.5} in eastern China (Huang et al., 2014; Yang et al., 2011). The acid
97 gases (i.e., NO_x, SO₂), together with NH₃, are crucial precursors of SIA via chemical
98 reactions that form particulate ammonium sulfate, ammonium bisulfate, and
99 ammonium nitrate (Ianniello et al., 2010). In addition to the adverse impacts on human
100 health via fine particulate matter formation (Liang et al., 2020; Kuerban et al., 2020),
101 large amounts of NH₃ and its aerosol-phase products also lead to nitrogen deposition
102 and consequently to environmental degradation (Ortiz-Montalvo et al., 2014; Zhan et
103 al., 2021).

104 Following the successful controls on NO_x and SO₂ emissions [since 2013 in China](#),
105 [some studies found SO₄²⁻ exhibited much larger decline than NO₃⁻ and NH₄⁺, which](#)
106 [lead to a rapid transition from sulfate-driven to nitrate-driven aerosol pollution \(Li et](#)
107 [al., 2019, 2021; Zhang et al., 2019\)](#). Attention is turning to NH₃ emissions as a possible
108 means of further PM_{2.5} control (Bai et al., 2019; Kang et al., 2016), particularly as

删除了: a

110 emissions of NH₃ increased between the 1980s and 2010s. Some studies have found
111 that NH₃ limited the formation of SIA in winter in the eastern United States (Pinder et
112 al., 2007) and Europe (Megaritis et al., 2013). Controls on NH₃ emissions have been
113 proposed in the TYAP, although mandatory measures and binding targets have not yet
114 been set (CSC, 2018b). Nevertheless, this proposal means that China will enter a new
115 phase of PM_{2.5} mitigation, with attention now given to both acid gas and NH₃ emissions.
116 However, in the context of effective control of PM_{2.5} pollution via its SIA component,
117 two key questions arise: 1) what are the responses of the constituents of SIA to
118 implementation of air pollution control policies, and 2) what is the relative efficiency
119 of NH₃ versus acid gas emission controls to reduce SIA pollution?

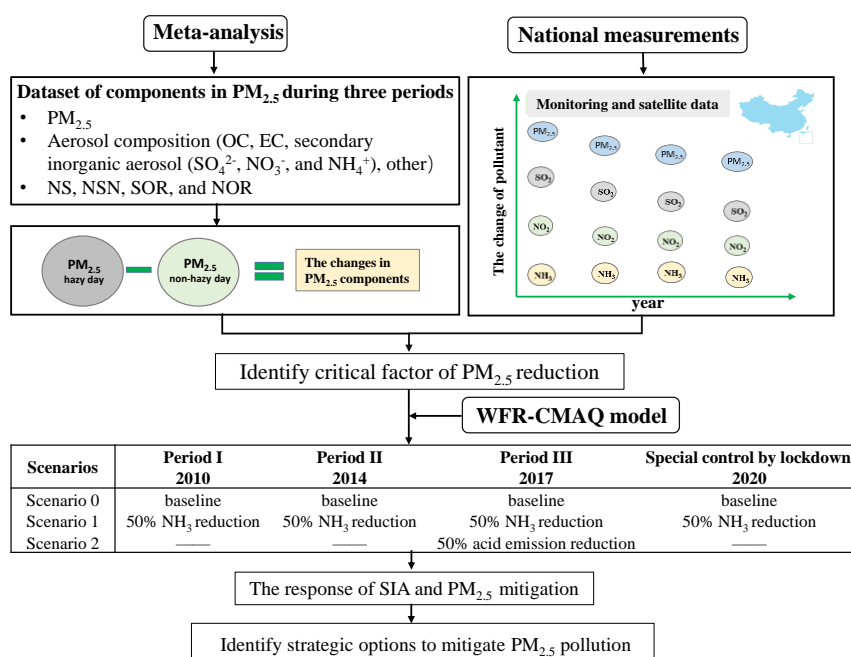
120 To fill this evidence gap and provide useful insights for policy-making to improve
121 air quality in China, this study adopts an integrated assessment framework. With respect
122 to the emission control policy summarized above, China's PM_{2.5} control can be divided
123 into three periods: period I (2000–2012), in which PM_{2.5} was not the targeted pollutant;
124 period II (2013–2016), the early stage of targeted PM_{2.5} control policy implementation;
125 and period III (2017–2019), the latter stage with more stringent policies. Therefore, our
126 research framework consists of two parts: (1) assessment of trends in annual mean
127 concentrations of PM_{2.5}, its chemical components and SIA gaseous precursors from
128 meta-analyses and observations; (2) quantification of SIA responses to emissions
129 reductions in NH₃ and acid gases using the Weather Research and Forecasting and
130 Community Multiscale Air Quality (WRF/CMAQ) models.

131 **2. Materials and methods**

132 **2.1. Research framework**

133 This study developed an integrated assessment framework to analysis the trends of
134 secondary inorganic aerosol and strategic options to reduce SIA and PM_{2.5} pollution in

135 China (Fig. 1). The difference in PM_{2.5} chemical components between hazy and non-
 136 hazy days was first assessed by meta-analysis of published studies. These were
 137 interpreted in conjunction with the trends in air concentrations of PM_{2.5} and its
 138 secondary inorganic aerosol precursors (SO₂, NO₂, and NH₃) derived from surface
 139 measurements and satellite observations. The potential of SIA and PM_{2.5} concentration
 140 reductions from precursor emission reductions was then evaluated using the Weather
 141 Research and Forecasting and Community Multiscale Air Quality (WRF/CMAQ)
 142 models.



143
 144 **Fig. 1.** Integrated assessment framework for Chinese PM_{2.5} mitigation strategic options.
 145 OC is organic carbon, EC is elemental carbon, NO₃⁻ is nitrate, SO₄²⁻ is sulfate, and NH₄⁺
 146 is ammonium. NS is the slope of the regression equation between [NH₄⁺] and [SO₄²⁻],
 147 NSN is the slope of the regression equation between [NH₄⁺] and [SO₄²⁻ + NO₃⁻], SOR
 148 is sulfur oxidation ratio, and NOR is nitrogen oxidation ratio. SIA is Secondary

149 inorganic aerosols. WRF-CMAQ is Weather Research and Forecasting and Community
150 Multiscale Air Quality models.

151 **2.2. Meta-analysis of PM_{2.5} and its chemical components**

152 Meta-analyses can be used to quantify the differences in concentrations of PM_{2.5} and
153 its secondary inorganic aerosol components (NH₄⁺, NO₃⁻, and SO₄²⁻) between hazy and
154 non-hazy days and to identify the major pollutants on non-hazy days (Wang et al.,
155 2019b); this provides evidence for effective options on control of precursor emissions
156 (NH₃, NO₂, and SO₂) for reducing occurrences of hazy days. To build a database of
157 atmospheric concentrations of PM_{2.5} and chemical components between hazy and non-
158 hazy days, we conducted a literature survey using the Web of Science and the China
159 National Knowledge Infrastructure for papers published between January 2000 and
160 January 2020. The keywords included: (1) "particulate matter," or "aerosol," or "PM_{2.5}"
161 and (2) "China" or "Chinese". Studies were selected based on the following conditions:
162 (1) Measurements were taken on both hazy and non-hazy days.
163 (2) PM_{2.5} chemical components were reported.
164 (3) If hazy days were not defined in the screened articles, the days with PM_{2.5}
165 concentrations > 75 µg m⁻³ (the Chinese Ambient Air Quality Standard Grade II for
166 PM_{2.5} (CSC, 2012)) were treated as hazy days.
167 (4) If an article reported measurements from different monitoring sites in the same city,
168 e.g. Mao et al. (2018) and Xu et al. (2019), then each measurement was considered an
169 independent study.
170 (5) If there were measurements in the same city for the same year, e.g. Tao et al. (2016)
171 and Han et al. (2017), then each measurement was treated as an independent study.

172 One hundred articles were selected based on the above conditions with the lists
173 provided in the Supporting Material dataset. For each selected study, we documented

174 the study sites, study periods, seasons, aerosol types, and aerosol species mass
175 concentrations (in $\mu\text{g m}^{-3}$) over the entire study period (2000–2019) (the detailed data
176 are provided in the dataset). In total, the number of sites contributing data to the meta-
177 analysis was 267 and their locations are shown in Fig. S1. If relevant data were not
178 directly presented in studies, a GetData Graph Digitizer (Version 2.25,
179 <http://www.getdatagraph-digitizer.com>) was used to digitize concentrations of PM_{2.5}
180 chemical components from figures. The derivations of other variables such as sulfur
181 and nitrogen oxidation ratios are described in Supplementary Information Method 1.

182 Effect sizes were developed to normalize the combined studies' outcomes to the
183 same scale. This was done through the use of log response ratios (lnRR) (Nakagawa et
184 al., 2012; Ying et al., 2019). The variations in aerosol species were evaluated as follows:

$$185 \ln RR = \ln \left(\frac{X_p}{X_n} \right) \quad (1)$$

186 where X_p and X_n represent the mean values of the studied variables of PM_{2.5} components
187 on hazy and non-hazy days, respectively. The mean response ratio was then estimated
188 as:

$$189 RR = \exp \left[\frac{\sum \ln RR(i) \times W(i)}{\sum W(i)} \right] \quad (2)$$

190 where $W(i)$ is the weight given to that observation as described below. Finally, variable-
191 related effects were expressed as percent changes, calculated as $(RR-1) \times 100\%$. A 95%
192 confidence interval not overlapping with zero indicates that the difference is significant.
193 A positive or negative percentage value indicates an increase or decrease in the response
194 variables, respectively.

195 We used inverse sampling variances to weight the observed effect size (RR) in the
196 meta-analysis (Benitez-Lopez et al., 2017). For the measurement sites where standard
197 deviations (SD) or standard errors (SE) were absent in the original study reports, we
198 used the "Bracken, 1992" approach to estimate SD (Bracken et al., 1992). The variation-

199 related chemical composition of PM_{2.5} was assessed by random effects in meta-analysis.
200 Rosenberg's fail safe-numbers (N_{fs}) were calculated to assess the robustness of findings
201 on PM_{2.5} to publication bias (Ying et al., 2019) (See Table S1). The results (effects)
202 were considered robust despite the possibility of publication bias if $N_{fs} > 5 \times n + 10$,
203 where n indicates the number of sites. The statistical analysis of the concentrations of
204 PM_{2.5} and secondary inorganic ions for three periods used a non-parametric statistical
205 method since concentrations were not normally distributed based on the Kruskal-Wallis
206 test (Kruskal and Walls, 1952). For each species, the Kruskal-Wallis one-way analysis
207 of variance (ANOVA) on ranks among three periods was performed with pairwise
208 comparison using Dunn's method (Dunn, 1964).

209 2.3. Data collection of air pollutant concentrations

210 To assess the recent annual trends in China of PM_{2.5} and of the SO₂ and NO₂
211 gaseous precursors to SIA, real-time monitoring data of these pollutants at 1498
212 monitoring stations in 367 cities during 2015–2019 were obtained from the China
213 National Environmental Monitoring Center (CNEMC) (<http://106.37.208.233:20035/>).
214 This is an open-access archive of air pollutant measurements from all prefecture-level
215 cities since January 2015. Successful use of data from CNEMC to determine
216 characteristics of air pollution and related health risks in China has been demonstrated
217 previously (Liu et al., 2016; Kuerban et al., 2020). The geography stations are shown
218 in Fig. S1. The annual mean concentrations of the three pollutants at all sites were
219 calculated from the hourly time-series data according to the method of Kuerban et al.
220 (2020). Information about sampling instruments, sampling methods, and data quality
221 controls for PM_{2.5}, SO₂, and NO₂ is provided in Supplementary Method 2. Surface NH₃
222 concentrations over China for the 2008–2016 (the currently available) were extracted
223 from the study of Liu et al. (2019a). Further details are in Supplementary Method 2.

224 2.4. WRF/CMAQ model simulations

225 The Weather Research and Forecasting model (WRFv3.8) and the Models-3
226 community multi-scale air quality (CMAQv5.2) model were used to evaluate the
227 impacts of emission reductions on SIA and PM_{2.5} concentrations over China. The
228 simulations were conducted at a horizontal resolution of 12 km × 12 km. The simulation
229 domain covered the whole of China, part of India and east Asia. In the current study,
230 focus was on the following four regions in China: Beijing-Tianjin-Hebei (BTH),
231 Yangtze River Delta (YRD), Pearl River Delta (PRD), and Sichuan Basin (SCB). The
232 model configurations used in this study were the same as those used in [Wu et al. \(2018a\)](#)
233 and are briefly described here. The WRFv3.8 model was applied to generate
234 meteorological inputs for the CMAQ model using the National Center for
235 Environmental Prediction Final Operational Global Analysis (NCEP-FNL) dataset
236 ([Morrison et al., 2009](#)). Default initial and boundary conditions were used in the
237 simulations. The carbon-bond (CB05) gas-phase chemical mechanism and AERO6
238 aerosol module were selected in the CMAQ configuration ([Guenther et al., 2012](#)).
239 Anthropogenic emissions for 2010, 2014 and 2017 were obtained from the Multi-
240 resolution Emission Inventory (<http://meicmodel.org>) with 0.25° × 0.25° spatial
241 resolution and aggregated to 12km×12km resolution ([Zheng et al., 2018](#); [Li et al., 2017](#)).
242 Each simulation was spun-up for six days in advance to eliminate the effects of the
243 initial conditions.

244 The years 2010, 2014 and 2017 were chosen to represent the anthropogenic
245 emissions associated with the periods I, II, III, respectively. January was selected as the
246 typical simulation month because wintertime haze pollution frequently occurs in this
247 month ([Wang et al., 2011](#); [Liu et al., 2019b](#)). [January of 2010 was also found to have](#)
248 [PM_{2.5} pollution more serious than other months](#) ([Geng et al., 2017, 2021](#)). The

删除了: The

删除了: the

删除了: an

252 sensitivity scenarios of emissions in January can therefore help to identify the efficient
253 option to control haze pollution.

254 The Chinese government has put a major focus on acid gas emission control
255 through a series of policies in the past three periods (Fig. S2). The ratio decreases of
256 anthropogenic emissions SO₂ and NO_x in January for the years 2010, 2014, 2017 and
257 2020 are presented in SI Tables S2 and S3, respectively. The emissions from
258 surrounding countries were obtained from the Emissions Database for Global
259 Atmospheric Research (EDGAR): HTAPV2. The scenarios and the associated
260 reductions of NH₃, NO_x and SO₂ for selected four years in three periods can be found
261 in Fig. 1.

262 The sensitivities of SIA and PM_{2.5} to NH₃ emissions reductions were determined
263 from the average PM_{2.5} concentrations in model simulations without and with an
264 additional 50% NH₃ emissions reduction. The choice of 50% additional NH₃ emissions
265 reduction is based on the feasibility and current upper bound of NH₃ emissions
266 reduction expected to be realized in the near future (Liu et al., 2019a; Zhang et al.,
267 2020a; Table S4). For example, Zhang et al. (2020a) found that the mitigation potential
268 of NH₃ emissions from cropland production and livestock production in China can
269 reach up to 52% and 58%, respectively. To eliminate the influences of varying
270 meteorological conditions, all simulations were conducted under the fixed
271 meteorological conditions of 2010.

272 During the COVID-19 lockdown in China, emissions of primary pollutants were
273 subject to unprecedented reductions due to national restrictions on traffic and industry;
274 in particular, emissions of NO_x and SO₂ reduced by 46% and 24%, respectively,
275 averaged across all Chinese provinces (Huang et al., 2021). We therefore also ran
276 simulations applying the same reductions in NO_x and SO₂ (based on 2017 MEIC) that

277 were actually observed during the COVID-19 lockdown as a case of special control in
278 2020.

279 **2.5 Model performance**

280 The CMAQ model has been extensively used in air quality studies (Zhang et al.,
281 2019; Backes et al., 2016) and the validity of the chemical regime in the CMAQ model
282 had been confirmed by our previous studies (Zhang et al., 2021a; Wang et al., 2020a,
283 2021a). In this study, we used surface measurements from previous publications (e.g.,
284 (Xiao et al., 2020, 2021; Geng et al., 2019; Xue et al., 2019) and satellite observations
285 to validate the modelling meteorological parameters by WRF model and air
286 concentrations of PM_{2.5} and associated chemical components by CMAQ model. The
287 meteorological measurements used for validating the WRF model performances were
288 obtained from the National Climate Data Center (NCDC)
289 (<ftp://ftp.ncdc.noaa.gov/pub/data/noaa/>). For validation of the CMAQ model, monthly
290 mean concentrations of PM_{2.5} were obtained from China High Air Pollutants (CHAP,
291 <https://weijing-rs.github.io/product.html>) database. We also collected ground-based
292 observations from previous publications to validate the modeling concentrations of
293 SO₄²⁻, NO₃⁻, and NH₄⁺. The detailed information of the monitoring sites is presented in
294 Table S5. Further information about the modelling is given in Supplementary Method
295 3 and Figs. S3-S7 and Table S5.

296 **3. Results and discussion**

297 **3.1. Characteristics of PM_{2.5} and its chemical components from the meta-analysis 298 and from nationwide observations**

299 The meta-analysis based on all published analyses of PM_{2.5} and chemical
300 component measurements during 2000–2019 reveals the changing characteristics of
301 PM_{2.5}. To assess the annual trends in PM_{2.5} and its major chemical components, we

删除了: Tracking Air pollution in

删除了: T

删除了: <http://tapdata.org.cn/>

305 made a three-period comparison using the measurements at sites that include both PM_{2.5}
306 and secondary inorganic ions SO₄²⁻, NO₃⁻, and NH₄⁺ (Fig. 2). The PM_{2.5} concentrations
307 on both hazy and non-hazy days showed no significant trend from period I to period II
308 based on the Kruskal-Wallis test. This can be explained by the enhanced atmospheric
309 oxidation capacity (Huang et al., 2021), faster deposition of total inorganic nitrate (Zhai
310 et al., 2021) and the changes of atmospheric circulation (Zheng et al., 2015; Li et al.,
311 2020). However, the observed concentrations of PM_{2.5} showed a downward trend from
312 Period I to Period III on the non-hazy days, decreasing by 8.2% (Fig. 2a), despite no
313 significant decreasing trend on the hazy days (Fig. 2a). In addition, the annual mean
314 PM_{2.5} concentrations from the nationwide measurements showed declining trends
315 during 2015-2019 averaged across all China and for each of the BTH, YRD, SCB, and
316 PRD megacity clusters of eastern China (Fig. 3a, d).

317 These results reflect the effectiveness of the pollution control policies (Fig. S2)
318 implemented by the Chinese government at the national scale. Nevertheless, PM_{2.5}
319 remained at relatively high levels. Over 2015–2019, the annual mean PM_{2.5}
320 concentrations at 74% of the 1498 sites (averaging 51.9 ± 12.4 μg m⁻³, Fig. 3a) exceeded
321 the Chinese Grade-II Standard (GB 3095–2012) of 35 μg m⁻³ (MEPC, 2012), indicating
322 that PM_{2.5} mitigation is a significant challenge for China.

删除了: and

设置了格式: 字体颜色: 自动设置

设置了格式: 字体颜色: 自动设置

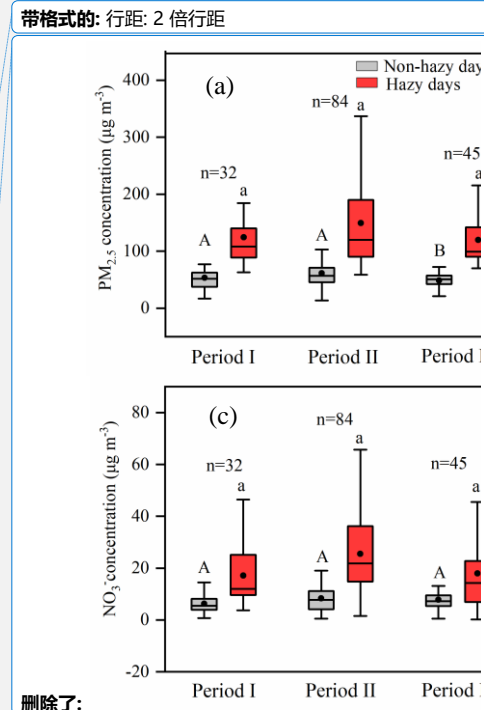
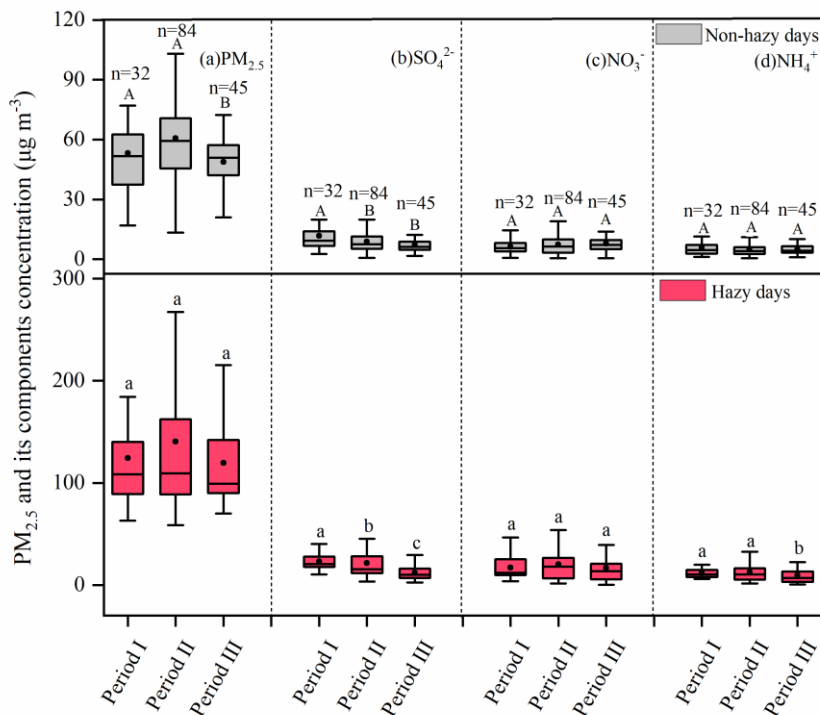
设置了格式: 字体颜色: 自动设置

设置了格式: 字体颜色: 自动设置

设置了格式: 字体颜色: 自动设置

设置了格式: 字体颜色: 自动设置

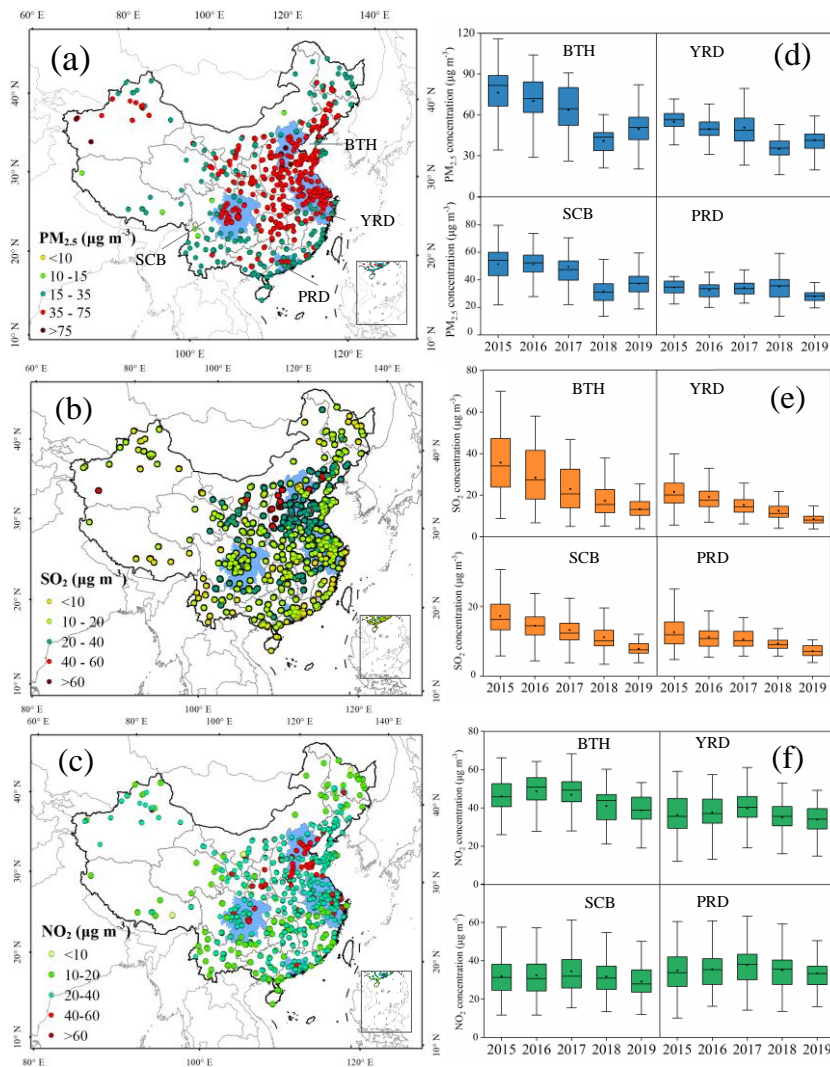
设置了格式: 字体颜色: 自动设置



324

325 **Fig. 2.** Comparisons of observed concentrations of (a) $\text{PM}_{2.5}$, (b) SO_4^{2-} , (c) NO_3^- , and
 326 (d) NH_4^+ between non-hazy and hazy days in Period I (2000–2012), Period II (2013–
 327 2016), and Period III (2017–2019). Bars with different letters denote significant
 328 differences among the three periods ($P < 0.05$) (upper and lowercase letters for non-
 329 hazy and hazy days, respectively). The upper and lower boundaries of the boxes
 330 represent the 75th and 25th percentiles; the line within the box represents the median
 331 value; the whiskers above and below the boxes represent the 90th and 10th percentiles;
 332 the point within the box represents the mean value. Comparison of the pollutants among
 333 the three-periods using Kruskal-Wallis and Dunn's test. The n represents independent
 334 sites; more detail on this is presented in [Section 2.2](#).

335



337

338 **Fig. 3.** Left: spatial patterns of annual mean observed concentration of (a) PM_{2.5}, (b)
 339 SO₂, (c) NO₂ at 1498 sites, averaged for 2015–2019. Right: the annual observed
 340 concentrations of (d) PM_{2.5}, (e) SO₂, and (f) NO₂ for 2015-2019 in four megacity
 341 clusters (BTH: Beijing-Tianjin-Hebei, YRD: Yangtze River Delta, SCB: Sichuan Basin,
 342 PRD: Pearl River Delta). The locations of the regions are indicated by the blue shading
 343 on the map. The upper and lower boundaries of the boxes represent the 75th and 25th

344 percentiles; the line within the box represents the median value; the whiskers above and
345 below the boxes represent the 90th and 10th percentiles; the point within the box
346 represents the mean value.

347 To further explore the underlying drivers of PM_{2.5} pollution, we analyzed the
348 characteristics of PM_{2.5} chemical components and their temporal changes in China. The
349 concentrations of PM_{2.5} and all its chemical components (except F⁻ and Ca²⁺) were
350 significantly higher on hazy days than on non-hazy days (Fig. 4A). Compared with
351 other components this difference was more significant for secondary inorganic ions (i.e.,
352 SO₄²⁻, NO₃⁻, and NH₄⁺). Sulfur oxidation ratio (SOR) and nitrogen oxidation ratio
353 (NOR) were also 58.0% and 94.4% higher on hazy days than on non-hazy days,
354 respectively, implying higher oxidations of gaseous species to sulfate- and nitrate-
355 containing aerosols on the hazy days (Sun et al., 2006; Xu et al., 2017).

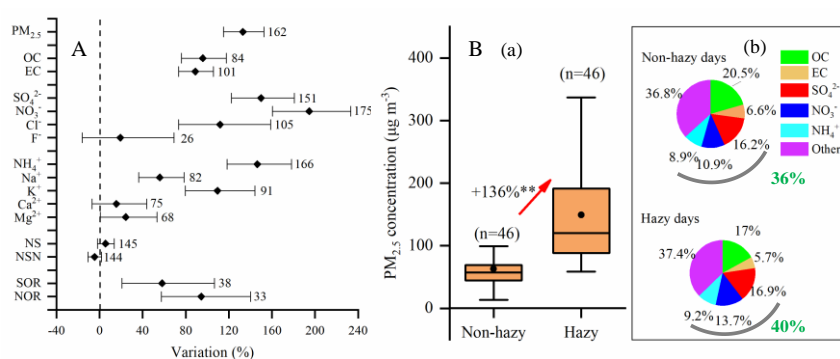
356 To provide quantitative information on differences in PM_{2.5} and its components
357 between hazy days and non-hazy days, we made a comparison using 46 groups of data
358 on simultaneous measurements of PM_{2.5} and chemical components. The 46 groups refer
359 to independent analyses from the literature that compare concentrations of PM_{2.5} and
360 major components (SO₄²⁻, NO₃⁻, NH₄⁺, OC, and EC) on hazy and non-hazy days

361 measured across different sets of sites. The “Other” species was calculated by
362 difference between PM_{2.5} and sum of OC, EC, and secondary inorganic ions (SO₄²⁻,
363 NO₃⁻ and NH₄⁺). As shown in Fig. 4B (a), PM_{2.5} concentrations significantly increased

364 (by 136%) on the hazy days ($149.2 \pm 81.6 \mu\text{g m}^{-3}$) relative to those on the non-hazy
365 days ($63.2 \pm 29.8 \mu\text{g m}^{-3}$). By contrast, each component's proportions within PM_{2.5}
366 differed slightly, with 36% and 40% contributions by SIA on non-hazy days and hazy
367 days, respectively (Fig. 4B(b)). This is not surprising because concentrations of PM_{2.5}
368 and SIA both significantly increased on the hazy days ($60.1 \pm 37.4 \mu\text{g m}^{-3}$ for SIA)

删除了:

370 relative to the non-hazy days ($22.4 \pm 12.1 \mu\text{g m}^{-3}$ for SIA). Previous studies have found
 371 that increased SIA formation is the major influencing factor for haze pollution in
 372 wintertime and summertime (mainly in years since 2013) in major Chinese cities in
 373 eastern China (Huang et al., 2014; Wang et al., 2019a; Li et al., 2018). Our results
 374 extend confirmation of the dominant role of SIA to $\text{PM}_{2.5}$ pollution over a large spatial
 375 scale in China and to longer temporal scales.



376 **Fig. 4.** (A) Variations in $\text{PM}_{2.5}$ concentration, aerosol component concentration, NS,
 377 NSN, SOR, and NOR from non-hazy to hazy days in China during 2000–2019. (B) (a)
 378 Summary of differences in $\text{PM}_{2.5}$ concentration between non-hazy and hazy days in
 379 China; (b) the average proportions of components of $\text{PM}_{2.5}$ on non-hazy and hazy days.
 380 NS is the slope of the regression equation between $[\text{NH}_4^+]$ and $[\text{SO}_4^{2-}]$, NSN is the slope
 381 of the regression equation between $[\text{NH}_4^+]$ and $[\text{SO}_4^{2-} + \text{NO}_3^-]$, SOR is sulfur oxidation
 382 ratio, and NOR is nitrogen oxidation ratio. The variations are considered significant if
 383 the confidence intervals of the effect size do not overlap with zero. ** denotes significant
 384 difference ($P < 0.01$) between hazy days and non-hazy days. The upper and lower
 385 boundaries of the boxes represent the 75th and 25th percentiles; the line within the box
 386 represents the median value; the whiskers above and below the boxes represent the 90th
 387 and 10th percentiles; the point within the box represents the mean value. Values
 388 adjacent to each confidence interval indicate number of measurement sites. The n
 389

390 represents independent sites; more detail on this is presented in [Section 2.2](#).

391 The effect values of SIA on the hazy days were significantly higher than those on
392 non-hazy days for all three periods (I, II, and III) ([Fig. 5](#)), indicating the persistent
393 prevalence of the SIA pollution problem over the past two decades. Considering
394 changes in concentrations, SO_4^{2-} showed a downward trend from Period I to Period III
395 on the non-hazy days and hazy day, decreasing by 38.6% and 48.3%, respectively ([Fig.](#)
396 [2b](#)). These results reflect the effectiveness of the SO_2 pollution control policies ([Ronald](#)
397 [et al., 2017](#)). In contrast, there were no significant downward trends in concentrations
398 of NO_3^- and NH_4^+ on either hazy or non-hazy days ([Fig. 2c, d](#)), but the mean NO_3^-
399 concentration in Period III decreased by 10.5% compared with that in Period II,
400 especially on hazy days (-16.8%). These results could be partly supported by decreased
401 NO_x emissions and tropospheric NO_2 vertical column densities between 2011 and 2019
402 in China owing to effective NO_x control policies ([Zheng et al., 2018](#); [Fan et al., 2021](#)).
403 The lack of significantly downward trends in NH_4^+ concentrations is due to the fact that
404 the total NH_3 emissions in China changed little and remained at high levels between
405 2000 and 2018, i.e., slightly decreased from 2000 (10.3 Tg) to 2012 (9.3 Tg) ([Kang et](#)
406 [al., 2016](#)) and then slightly increased between 2013 and 2018 ([Liu et al., 2021](#)). The
407 same trends are also found in Quzhou in China, which is a long-term in situ monitoring
408 site (in Quzhou County, North China Plain, operated by our group) during the period
409 2012-2020 from previous publications ([Xu et al., 2016](#); [Zhang et al., 2021b](#), noted that
410 data during 2017-2020 are unpublished before) ([Fig. S8](#)). [Zhang et al. \(2020b\)](#) found
411 that the clean air actions implemented in 2017 effectively reduced wintertime
412 concentrations of PM_{10} (particulate matter with diameter $\leq 10 \mu\text{m}$), SO_4^{2-} and NH_4^+ in
413 Beijing compared with those in 2007, but had no apparent effect on NO_3^- . [Li et al.](#)

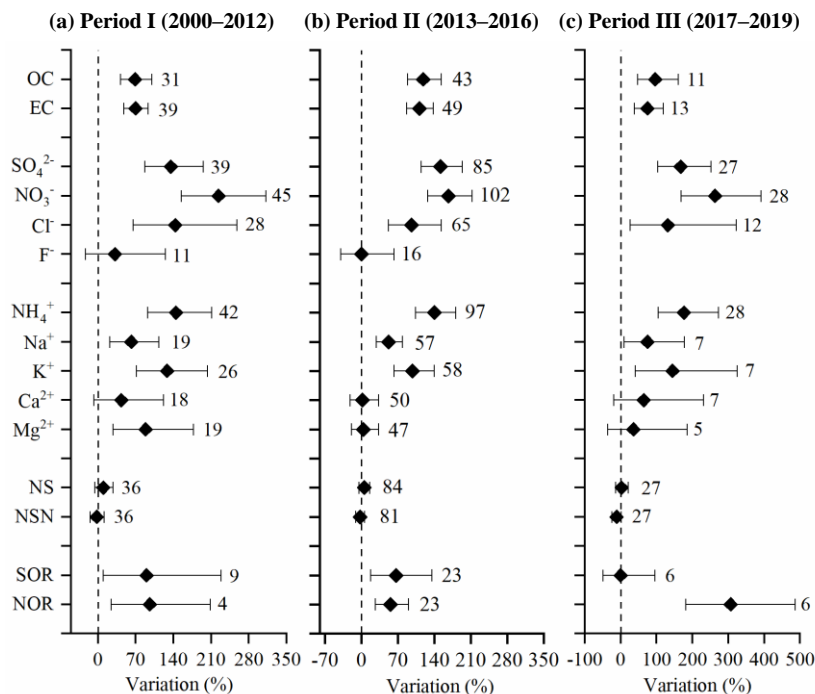
414 (2021) also found that SO_4^{2-} exhibited a significant decline. However, NO_3^- did not
415 evidently exhibit a decreasing trend in the BTH region.

删除了: o

删除了: n exhibit an evident

416 Our findings are to some extent supported by the nationwide measurements.
417 Annual mean SO_2 concentrations displayed a clear decreasing trend with a 53%
418 reduction in 2019 relative to 2015 for the four megacity clusters of eastern China (Fig.
419 3b, e), whereas there were only slight reductions in annual mean NO_2 concentrations
420 (Fig. 3c, f). In contrast, annual mean NH_3 concentrations showed an obvious increasing
421 trend in in both northern and southern regions of China, and especially in the BTH
422 region (Fig. S9).

423 Overall, the above analyses indicate that SO_4^{2-} concentrations responded
424 positively to air policy implementations at the national scale, but that reducing NO_3^-
425 and NH_4^+ remains a significant challenge. China has a history of around 10-20 years
426 for SO_2 and NO_x emission control and has advocated NH_3 controls despite to date no
427 mandatory measures and binding targets having been set (Fig. S2). Nevertheless, $\text{PM}_{2.5}$
428 pollution, especially SIA such as NO_3^- and NH_4^+ , is currently a serious problem (Fig. 4
429 and 5a, b). Some studies have reported that $\text{PM}_{2.5}$ pollution can be effectively reduced
430 if implementing synchronous NH_3 and NO_x/SO_2 controls (Liu et al., 2019b). Therefore,
431 based on the above findings, we propose that NH_3 and NO_x/SO_2 emission mitigation
432 should be simultaneously strengthened to mitigate haze pollution.



435
 436 **Fig. 5.** Variations in PM_{2.5} composition, NS, NSN, SOR, and NOR from non-hazy to
 437 hazy days in (a) Period I (2000–2012), (b) Period II (2013–2016), (c) Period III (2017–
 438 2019). NS is the slope of the regression equation between [NH₄⁺] and [SO₄²⁻], NSN is
 439 the slope of the regression equation between [NH₄⁺] and [SO₄²⁻ + NO₃⁻], SOR is sulfur
 440 oxidation ratio, and NOR is nitrogen oxidation ratio. The variations are statistically
 441 significant if the confidence intervals of the effect size do not overlap with zero. Values
 442 adjacent to each confidence interval indicate number of measurement sites. The *n*
 443 represents independent sites; more detail on this is presented in Section 2.2.

444 3.2. Sensitivities from model simulations

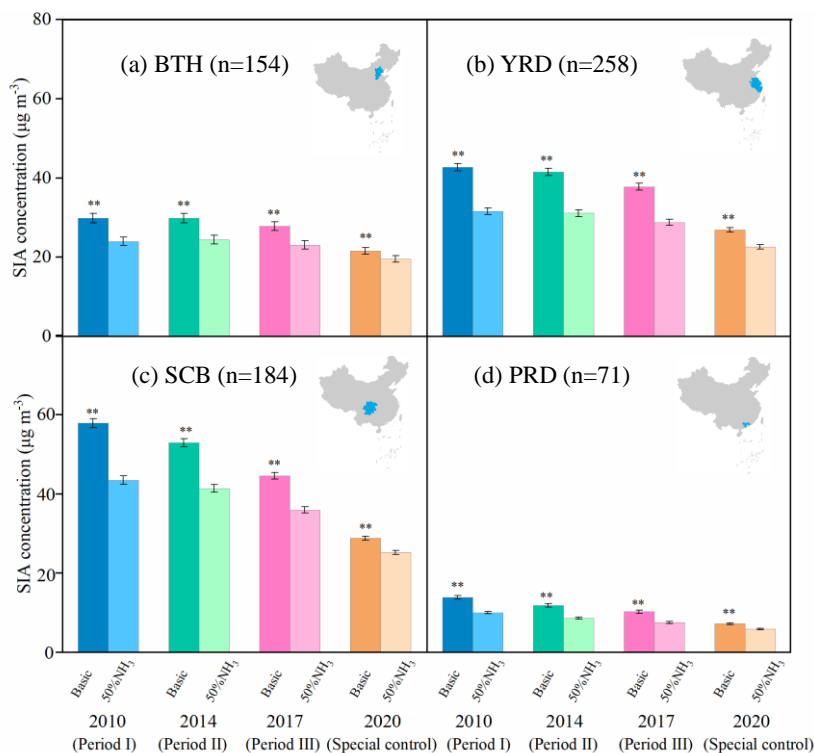
445 To further examine the efficiencies of NH₃ and acid gas emission reductions on
 446 SIA and PM_{2.5} mitigation, the decreases of mean SIA and PM_{2.5} concentrations with and
 447 without additional 50% NH₃ reductions were simulated using the WRF/CMAQ model.

448 Fig. 6 and Fig S10 shows that, compared to 2010, SIA and PM_{2.5} concentrations in
449 January in 2017 were significantly decrease in the BTH, YRD, SCB, and PRD megacity
450 clusters, respectively, in the simulations without additional NH₃ emission reductions.
451 Across the four megacity clusters, the reduction in SIA and PM_{2.5} is largest in the SCB
452 region from 2010 to 2017 and smallest in the PRD region.

453 When simulating the effects of an additional 50% NH₃ emissions reductions in
454 January in each of the years 2010, 2014 and 2017, the SIA concentrations in the BTH,
455 YRD, SCB and PRD megacity clusters decreased by $25.9 \pm 0.3\%$, $24.4 \pm 0.3\%$, and
456 $22.9 \pm 0.3\%$, respectively (Fig. 6, Fig. S11, and Table S6). The reductions of PM_{2.5} in
457 2010, 2014 and 2017 were $9.7 \pm 0.1\%$, $9.0 \pm 0.1\%$, and $9.2 \pm 0.2\%$ in the megacity clusters,
458 respectively. (Figs. S10 and S12). Whilst these results confirm the effectiveness of NH₃
459 emission controls, it is important to note that the response of SIA concentrations is less
460 sensitive to additional NH₃ emission controls along the timeline of the SO₂ and NO_x
461 anthropogenic emissions reductions associated with the series of clean air actions
462 implemented by the Chinese government from 2010 to 2017 (Zheng et al., 2018). Given
463 the feasibility and current upper bound of NH₃ emission reductions options in the near
464 future (50%) (Liu et al., 2019b), further abatement of SIA concentrations merely by
465 reducing NH₃ emissions is limited in China. In other words, the controls on acid gas
466 emissions should continue to be strengthened beyond their current levels.

467

删除了: and



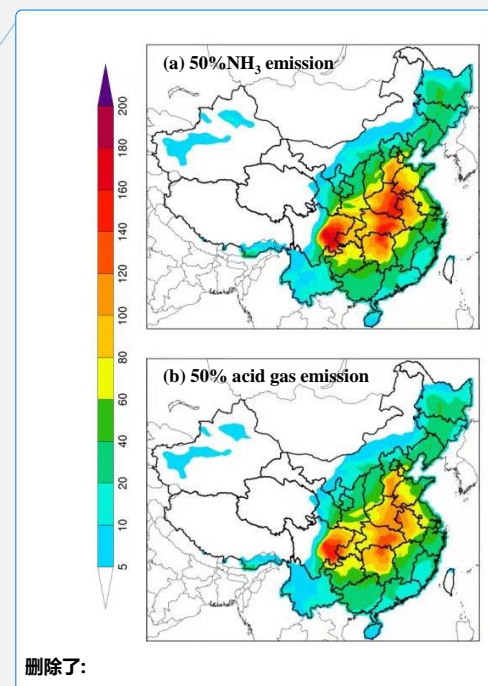
469

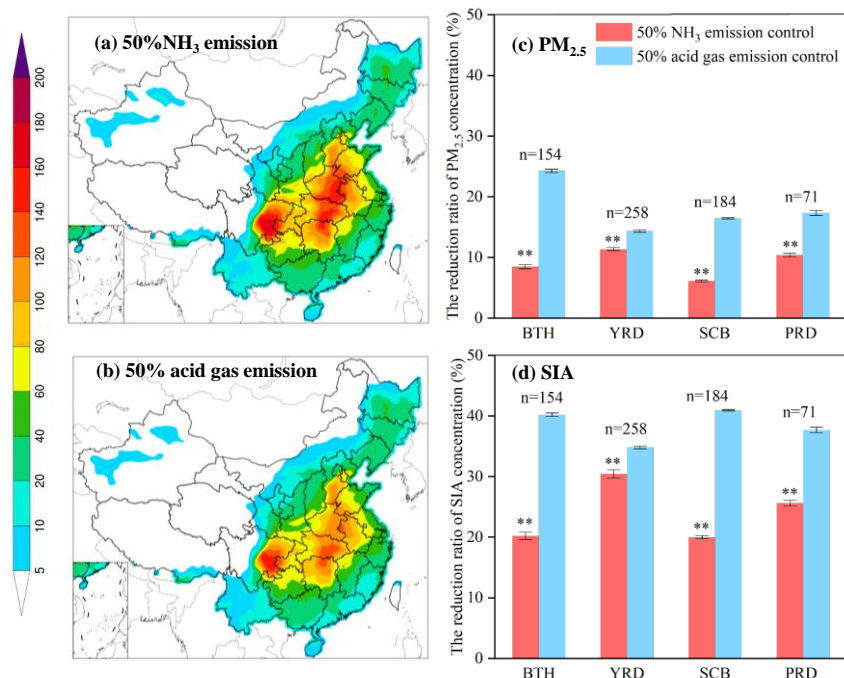
470 **Fig. 6.** Simulated SIA concentrations (in $\mu\text{g m}^{-3}$) without (basic) and with 50%
 471 ammonia (NH_3) emissions reductions in January for the years 2010, 2014, 2017 and
 472 2020 in four megacity clusters (BTH: Beijing-Tianjin-Hebei, YRD: Yangtze River
 473 Delta, SCB: Sichuan Basin, PRD: Pearl River Delta). Inset maps indicate the location
 474 of each region. ** denotes significant difference without and with 50% ammonia
 475 emission reductions ($P < 0.05$). n is the number of calculated samples by grid extraction.
 476 Error bars are standard errors of means. (Period I (2000–2012), Period II (2013–2016),
 477 and Period III (2017–2019); Special control is the restrictions in economic activities
 478 and associated emissions during the COVID-19 lockdown period in 2020.)

479 To further verify the above findings, we used the reductions of emissions of acid
 480 gases (46% and 23% for NO_x and SO_2 , respectively, in the whole China) during the

481 COVID-lockdown period as a further scenario (Huang et al., 2021). The model
482 simulations suggest that the effectiveness of reductions in SIA and PM_{2.5} concentrations
483 by a 50% NH₃ emission reduction further declined in 2020 ($15 \pm 0.2\%$ for SIA, and
484 $5.1 \pm 0.2\%$ for PM_{2.5}), but the resulting concentrations of them were lower ($20.8 \pm 0.3\%$
485 for SIA, and $15.6 \pm 0.3\%$ for PM_{2.5}) when compared with that in 2017 under the same
486 scenario of an additional 50% NH₃ emissions reduction (and constant meteorological
487 conditions) (Fig. 6 and Table S6), highlighting the importance of concurrently NH₃
488 mitigation when acid gas emissions are strengthened. To confirm the importance of acid
489 gas emissions, another sensitivity simulation was conducted for 2017, in which the acid
490 gas (NO_x and SO₂) emissions were reduced by 50% (Fig. 7). We found that reductions
491 in SIA concentrations are $13.4 \pm 0.5\%$ greater for the 50% reductions in SO₂ and NO_x
492 emissions than for the 50% reductions in NH₃ emissions. These results indicate that to
493 substantially reduce SIA pollution it remains imperative to strengthen emission controls
494 on NO_x and SO₂ even when a 50% reduction in NH₃ emission is targeted and achieved.

495





497
 498 **Fig. 7.** Left: the spatial distributions of simulated PM_{2.5} concentrations (in $\mu\text{g m}^{-3}$) in
 499 January 2017 with (a) 50% reductions in ammonia (NH₃) emissions and (b) 50%
 500 reductions in acid gas (NO_x and SO₂) emissions. Right: the % decreases in PM_{2.5} (c)
 501 and SIA (d) concentrations for the simulations with compared to without the NH₃ and
 502 acid gas emissions reductions in four megacity clusters (BTH: Beijing-Tianjin-Hebei,
 503 YRD: Yangtze River Delta, SCB: Sichuan Basin, PRD: Pearl River Delta). ** denotes
 504 significant differences without and with 50% ammonia emission reductions ($P < 0.05$).
 505 n is the number of calculated samples by grid extraction. Error bars are standard errors
 506 of means.

507 3.3. Uncertainty analysis and limitations

508 Some limitations should be noted in interpreting the results of the present study: this
 509 study examined period-to-period changes in PM_{2.5} chemical components based on a

510 meta-analysis and the efficiencies of NH_3 and acid gas emission reductions on $\text{PM}_{2.5}$
511 mitigation. Some uncertainties may still exist in meta-analysis of nationwide
512 measurements owing to differences in monitoring, sample handling and analysis
513 methods as well as lack of long-term continuous monitoring sites (Fig. 2). For example,
514 the measurements of $\text{PM}_{2.5}$ were mainly taken using the TEOM method, which is
515 associated with under-reading of PM due to some nitrate volatilization at its operational
516 temperature. To test whether the use of data during 2000–2019 could bias annual trends
517 of $\text{PM}_{2.5}$ and chemical components, we summarize measurements of $\text{PM}_{2.5}$ at a long-
518 term monitoring site (in Quzhou County, North China Plain, operated by our group)
519 during the period 2012-2020 from previous publications (Xu et al., 2016; Zhang et al.,
520 2021b, noted that data during 2017-2020 are unpublished before). The $\text{PM}_{2.5}$ and SO_4^{2-}
521 show the same decreasing trend. The concentration of NO_3^- and NH_4^+ do not show
522 significant change (Fig. S8). The results are consistent with the trend for the whole of
523 China obtained from the meta-analysis. Considering the uncertainty of $\text{PM}_{2.5}$ and its
524 major components between different seasons (winter, summer, etc) and site type (urban,
525 suburban or rural). We have analyzed historic trend in the different season and sites
526 (Figs. S13-S20). We found that concentrations of $\text{PM}_{2.5}$ and its major chemical
527 components (SO_4^{2-} , NO_3^- , and NH_4^+) were significantly higher in fall and winter than
528 in spring and summer (Fig. S13). Only the winter season showed significant change
529 trend in the three periods (Figs. S14-S17). The analyses also confirmed that pollution
530 days predominated in winter. We also found that concentrations of $\text{PM}_{2.5}$ and its major
531 chemical components were higher at urban than rural sites (Fig. S18). Spatially, the
532 trends of $\text{PM}_{2.5}$ and its major components are similar across the whole of China (both
533 of urban and rural) (Fig. S19). Rural areas show the same change trend in hazy days
534 compared with whole of China (Fig. S20).

535 WRF-CMAQ model performance also has some uncertainty. We performed the
536 validations of WRF and CMAQ models. The simulations of temperature at 2 m above
537 ground (T2), wind speed (WS), and relative humidity (RH) versus observed values at
538 400 monitoring sites in China are shown in Fig. S7. The meteorological measurements
539 were obtained from the National Climate Data Center (NCDC)
540 (<ftp://ftp.ncdc.noaa.gov/pub/data/noaa/>). The comparisons showed that the model
541 performed well at predicting meteorological parameters with R values of 0.94, 0.64 and
542 0.82 for T2, WS and RH, respectively. However, the WS was overestimated (22.3%
543 NMB) in most regions of China, which is also reported in previous studies (Gao et al.,
544 2016; Chen et al., 2019). This may be related to the underlying surface parameters set
545 in the WRF model configurations.

546 In addition, the simulations of PM_{2.5} and associated chemical components by the
547 CMAQ model have potential biases in the spatial pattern, although the CMAQ model
548 has been extensively used in air quality studies (Backes et al., 2016; Zhang et al., 2019)
549 and the validity of the chemical regime in the CMAQ model had been confirmed by
550 our previous studies (Zhang et al., 2021a; Wang et al., 2020a, 2021a). Since nationwide
551 measurements of PM_{2.5} and associated chemical components are lacking in 2010 in
552 China, we undertook our own validation of PM_{2.5} and its components (such as SO₄²⁻,
553 NO₃⁻, and NH₄⁺) using a multi-observation dataset that includes those monitoring data
554 and satellite observations at a regional scale that were available.

555 First, the simulated monthly mean PM_{2.5} concentration in January 2010 was
556 compared with corresponding data obtained from the [China High Air Pollutants \(CHAP,](#)
557 <https://weijing-rs.github.io/product.html>) database. The satellite historical PM_{2.5}
558 predictions are reliable (average $R^2 = 0.80$ and RMSE = 11.26 $\mu\text{g m}^{-3}$) using cross
559 validation against the in-situ surface observations on a monthly basis (Wei et al., 2020,

删除了: Tracking Air pollution in China (TAP,
<http://tapdata.org.cn/>)

删除了: in a

563 2021). The model well captured the spatial distributions of PM_{2.5} concentrations in our
564 studied regions of BTH, YRD, PRD, and SCB (Fig. S3a), with correlation coefficient
565 (*R*) between simulated and satellite observed PM_{2.5} concentrations of 0.96, 0.80, 0.60,
566 and 0.85 for BTH, YRD, PRD, and SCB, respectively.

567 Second, we also collected ground-based observations from previous publications
568 (Xiao et al., 2020, 2021; Geng et al., 2019; Xue et al., 2019) to validate the modeling
569 concentrations of SO₄²⁻, NO₃⁻, and NH₄⁺. Detailed information about the monitoring
570 sites is presented in Table S5. The distributions of the simulated monthly mean
571 concentrations of SO₄²⁻, NO₃⁻, and NH₄⁺ in January 2010 over China is compared with
572 collected surface measurements are shown in Fig. S4a, b, and c, respectively, with their
573 linear regression analysis presented in Fig. S4d. The model showed underestimation in
574 simulating SO₄²⁻ and NO₃⁻ in the BTH region, which might be caused by the uncertainty
575 in the emission inventory. The lack of heterogeneous pathways for SO₄²⁻ formation in
576 the CMAQ model might also be an important reason for the negative bias between
577 simulations and measurements (Yu et al., 2005; Cheng et al., 2016). The model
578 overestimated NO₃⁻ concentration in the SCB region, but can capture the spatial
579 distribution of NO₃⁻ in other regions. The overestimation of NO₃⁻ has been a common
580 problem in regional chemical transport models such as CMAQ, GEOS-CHEM and
581 CAMx (Yu et al., 2005; Fountoukis et al., 2011; Zhang et al., 2012; Wang et al., 2013),
582 due to the difficulties in correctly capturing the gas and aerosol-phase nitrate
583 partitioning (Yu et al., 2005). The modeling of NH₄⁺ concentrations show good
584 agreement with the observed values. Generally, the evaluation results indicate that the
585 model reasonably predicted concentrations of SO₄²⁻, NO₃⁻, and NH₄⁺ in PM_{2.5}.

586 Third, we performed a comparison of the time-series of the observed and simulated
587 hourly PM_{2.5} and its precursors (SO₂ and NO₂) during January 2010. The model well

588 captures the temporal variations of the PM_{2.5} in Beijing, with an NMB value of 0.05 ug
589 m⁻³, NME of 28%, and *R* of 0.92 (Fig. 5a). The predicted daily concentrations of NO₂
590 and SO₂ during January 2010 also show good agreement with the ground measurements
591 in Beijing, with NMB and *R* values of 0.12 $\mu\text{g m}^{-3}$ and 0.89 for NO₂, and -0.04, 0.95
592 for SO₂, respectively (Fig. 5b). The variations of daily PM_{2.5} concentrations between
593 simulation and observation at 4 monitoring sites (Shangdianzi, Chengdu, Institute of
594 Atmospheric Physics, Chinese Academy of Sciences (IAP-CAS), and Tianjin) from 14
595 to 30 January 2010 also matched well, with NMB values ranging from -0.05 to 0.12 ug
596 m⁻³, and *R* values exceeding 0.89 (Fig. S5c).

597 We also compared the simulated and observed concentrations of PM_{2.5}, NO₂, and
598 SO₂ in China in pre-COVID period (1–26 January 2020) and during the COVID-
599 lockdown period (27 January–26 February) with actual meteorological conditions. As
600 shown in Fig. S6, both the simulations and observations suggested that the PM_{2.5} and
601 NO₂ concentrations substantially decreased during the COVID-lockdown, mainly due
602 to the sharp reduction in vehicle emissions (Huang et al., 2021; Wang et al., 2021b).
603 For SO₂, the concentrations decreased very little and even increased at some monitoring
604 sites. The model underestimated the concentrations of PM_{2.5}, NO₂, and SO₂, with NMB
605 values of -21.4%, -22.1%, and -9.6%, respectively. We also newly evaluated the model
606 performance in actual meteorological conditions for PM_{2.5} concentrations in January
607 2014 and 2017, respectively. As shown in the Figure S21, the model well captured the
608 spatial distribution of PM_{2.5} concentration in China with MB (NMB) values of 23.2 μg
609 m⁻³ (15.4%) and 26.8 $\mu\text{g m}^{-3}$ (-26.7%) for 2014 and 2017, respectively. The simulated
610 PM_{2.5} concentrations compared well against the observations, with *R* values of 0.82 and
611 0.65, respectively

删除了: This phenomenon is reasonable as the simulations for the two periods in 2020 used the meteorology for 2010 whereas measured changes are strongly influenced by the actual meteorological conditions.

617 **3.4. Implication and outlook**

618 Improving air quality is a significant challenge for China and the world. A key
619 target in China is for all cities to attain annual mean $PM_{2.5}$ concentrations of $35 \mu g m^{-3}$
620 or below by 2035 (Xing et al., 2021). However, this study has shown that 74% of 1498
621 nationwide measurement sites have exceeded this limit value in recent years (averaged
622 across 2015-2019). Our results indicated that acid gas emissions still need to be a focus
623 of control measures, alongside reductions in NH_3 emissions, in order to reduce SIA (or
624 $PM_{2.5}$) formation. Model simulations for the month of January underpin the finding that
625 the relative effectiveness of NH_3 emission control decreased over the period from 2010
626 to 2017. However, simulating the substantial emission reductions in acid gases due to
627 the lockdown during the COVID-19 pandemic, with fossil fuel-related emissions
628 reduced to unprecedented levels, indicated the importance of ammonia emission
629 abatement for $PM_{2.5}$ air quality improvements when SO_2 and NO_x emissions have
630 already reached comparatively low levels. Therefore, a strategic and integrated
631 approach to simultaneously undertaking acid gas emissions and NH_3 mitigation is
632 essential to substantially reduce $PM_{2.5}$ concentrations. However, the mitigation of acid
633 gas and NH_3 emissions pose different challenges due to different sources they originate
634 from.

635 The implementation of further reduction of acid gas emissions is challenging. The
636 prevention and control of air pollution in China originally focused on the control of acid
637 gas emissions (Fig. S2). The controls have developed from desulfurization and
638 denitrification technologies in the early stages to advanced end-of-pipe control
639 technologies. By 2018, over 90% of coal-fired power plants had installed end-of-pipe
640 control technologies (CEC, 2020). The potential for further reductions in acid gas
641 emissions by end-of-pipe technology might therefore be limited. Instead, addressing

642 total energy consumption and the promotion of a transition to clean energy through a
643 de-carbonization of energy production is expected to be an inevitable requirement for
644 further reducing PM_{2.5} concentrations (Xing et al., 2021). In the context of improving
645 air quality and mitigating climate change, China is adopting a portfolio of low-carbon
646 policies to meet its Nationally Determined Contribution pledged in the Paris Agreement.
647 Studies show that if energy structure adjusts and energy conservation measures are
648 implemented, SO₂ and NO_x will be further reduced by 34% and 25% in Co-Benefit
649 Energy scenario compared to the Nationally Determined Contribution scenario in 2035
650 (Xing et al., 2021). Although it has been reported that excessive acid gas emission
651 controls may increase the oxidizing capacity of the atmosphere and increase other
652 pollution, PM_{2.5} concentrations have consistently decreased with previous acid gas
653 control (Huang et al., 2021). In addition, under the influence of low-carbon policies,
654 other pollutant emissions will also be controlled. Opportunities and challenges coexist
655 in the control of acid gas emissions.

656 In contrast to acid gas emissions, NH₃ emissions predominantly come from
657 agricultural sources. Although the Chinese government has recognized the importance
658 of NH₃ emissions controls in curbing PM_{2.5} pollution, NH₃ emissions reductions have
659 only been proposed recently as a strategic option and no specific nationwide targets
660 have yet been implemented (CSC, 2018b). The efficient implementation of NH₃
661 reduction options is a major challenge because NH₃ emissions are closely related to
662 food production, and smallholder farming is still the dominant form of agricultural
663 production in China. The implementation of NH₃ emissions reduction technologies is
664 subject to investment in technology, knowledge and infrastructure, and most farmers
665 are unwilling or economically unable to undertake additional expenditures that cannot
666 generate financial returns (Gu et al., 2011; Wu et al., 2018b). Therefore, economically

667 feasible options for NH₃ emission controls need to be developed and implemented
668 nationwide.

669 We propose the following three requirements that need to be met to achieve
670 effective reductions of SIA concentrations and hence of PM_{2.5} concentrations in China.

671 First, binding targets to reduce both NH₃ and acid gas emissions should be set. The
672 targets should be designed to meet the PM_{2.5} standard, and NH₃ concentrations should
673 be incorporated into the monitoring system as a government assessment indicator. In
674 this study, we find large differences in PM_{2.5} concentration reductions from NH₃
675 emissions reduction in the four megacity regions investigated. At a local scale (i.e., city
676 or county), the limiting factors may vary within a region (Wang et al., 2011). Thus,
677 local-specific environmental targets should be considered in policy-making.

678 Second, further strengthening of the controls on acid gas emissions are still needed,
679 especially under the influence of low-carbon policies, to promote emission reductions
680 and the adjustment of energy structures and conservation. Ultra-low emissions should
681 be requirements in the whole production process, including point source emissions,
682 diffuse source emissions, and clean transportation (Xing et al., 2021; Wang et al.,
683 2021a). The assessment of the impact of ultra-low emissions is provided in Table S7.
684 In terms of energy structure, it is a requirement to eliminate outdated production
685 capacity and promote low-carbon new energy generation technologies.

686 Third, a requirement to promote feasible NH₃ reduction options throughout the
687 whole food production chain, for both crop and animal production. Options include the
688 following. 1) Reduction of nitrogen input at source achieved, for example, through
689 balanced fertilization based on crop needs instead of over-fertilization, and promotion
690 of low-protein feed in animal breeding. 2) Mitigation of NH₃ emissions in food
691 production via, for example, improved fertilization techniques (such as enhanced-

删除了: 6

693 efficiency fertilizer (urease inhibitor products), fertilizer deep application, fertilization-
694 irrigation technologies (Zhan et al., 2021), and coverage of solid and slurry manure. 3)
695 Encouragement for the recycling of manure back to croplands, and reduction in manure
696 discarding and long-distance transportation of manure fertilizer. Options for NH₃
697 emissions control are provided in Table S4. Although the focus here has been on
698 methods to mitigate NH₃ emissions, it is of course critical simultaneously to minimize
699 N losses in other chemical forms such as nitrous oxide gas emissions and aqueous
700 nitrate leaching (Shang et al., 2019; Wang et al., 2020b).

701 4. Conclusions

702 The present study developed an integrated assessment framework using meta-
703 analysis of published literature results, analysis of national monitoring data, and
704 chemical transport modelling to provide insight into the effectiveness of SIA precursor
705 emissions controls in mitigating poor PM_{2.5} air quality in China. We found that PM_{2.5}
706 concentration significantly decreased in 2000-2019 due to acid gas control policies, but
707 PM_{2.5} pollution still severe. Compared with other components, this difference was more
708 significant higher (average increase 98%) for secondary inorganic ions (i.e., SO₄²⁻, NO₃⁻,
709 and NH₄⁺) on hazy days than on-hazy days. This is mainly caused by the persistent SIA
710 pollution during the same period. with sulfate concentrations significantly decreased
711 and no significant changes observed for nitrate and ammonium concentrations. The
712 reductions of SIA concentrations in January in megacity clusters of eastern China by
713 additional 50% NH₃ emission controls decreased from 25.9 ± 0.3% in 2010 to 22.9 ±
714 0.3% in 2017, and to 15 ± 0.2% in the COVID lockdown in 2020 for simulations
715 representing reduced acid gas emissions to unprecedented levels, but the SIA
716 concentrations decreased by 20.8 ± 0.3% in 2020 compared with that in 2017 under the
717 same scenario of an additional 50% NH₃ emissions reduction. In addition, the reduction

718 of SIA concentration in 2017 was $13.4 \pm 0.5\%$ greater for 50% acid gas (SO_2 and NO_x)
719 reductions than for the NH_3 emissions reduction. These results indicate that acid gas
720 emissions need to be further controlled concertedly with NH_3 reductions to substantially
721 reduce $\text{PM}_{2.5}$ pollution in China.

722 Overall, this study provides new insight into the responses of SIA concentrations
723 in China to past air pollution control policies and the potential balance of benefits in
724 including NH_3 emissions reductions with acid gas emissions controls to curb SIA
725 pollution. The outcomes from this study may also help other countries seeking feasible
726 strategies to mitigate $\text{PM}_{2.5}$ pollution.

727

728

729 **Data availability**

730 All data in this study are available from the from the corresponding authors (Wen Xu,
731 wenxu@cau.edu.cn; Shaocai Yu, shaocaiyu@zju.edu.cn) upon request.

732 **Author contributions**

733 W.X., S.Y., and F.Z. designed the study. F.M., Y.Z., W.X., and J.K. performed the
734 research. F.M., Y.Z., W.X., and J.K. analyzed the data and interpreted the results. Y.Z.
735 conducted the model simulations. L.L. provided satellite-derived surface NH_3
736 concentration. F.M., W.X., Y.Z., and M.R.H. wrote the paper, S. R., M.W., K.W., J.K.,
737 Y.Z., Y.H., P.L., J.W., Z.C., X.L., M.R.H., S.Y. and F.Z. contributed to the discussion
738 and revision of the paper.

739 **Declaration of Competing Interest**

740 The authors declare that they have no known competing financial interests or personal
741 relationships that could have appeared to influence the work reported in this paper.

742 **Acknowledgments**

743 This study was supported by National Natural Science Foundation of China (42175137,
744 21577126 and 41561144004), China Scholarship Council (No.201913043), the
745 National Key Research and Development Program of China (2021YFD1700900), the
746 Department of Science and Technology of China (No. 2016YFC0202702,
747 2018YFC0213506 and 2018YFC0213503), National Research Program for Key Issues
748 in Air Pollution Control in China (No. DQGG0107), and the High-level Team Project
749 of China Agricultural University. SR's contribution was supported by the Natural
750 Environment Research Council award number NE/R000131/1 as part of the SUNRISE
751 program delivering National Capability.

752 **References**

- 753 An, Z. S., Huang, R. J., Zhang, R.Y., Tie, X. X., Li, G. H., Cao, J. J., Zhou, W. J., Shi,
754 Z. G., Han, Y. M., Gu, Z. L., and Ji, Y. M.: Severe haze in northern China: A
755 synergy of anthropogenic emissions and atmospheric processes, *Proc. Natl. Acad.*
756 *Sci. U. S. A.*, 116, 8657-8666. <https://doi.org/10.1073/pnas.1900125116>, 2019.
- 757 Backes, A., Aulinger, A., Bieser, J., Matthias, V., and Quante, M.: Ammonia emissions
758 in Europe, part II: How ammonia emission abatement strategies affect secondary
759 aerosols, *Atmos. Environ.*, 126, 153-161,
760 <https://doi.org/10.1016/j.atmosenv.2015.11.039>, 2016.
- 761 Bai, Z., Winiwarter, W., Klimont, Z., Velthof, G., Misselbrook, T., Zhao, Z., Jin, X.,
762 Oenema, O., Hu, C., and Ma, L.: Further improvement of air quality in China needs
763 clear ammonia mitigation target, *Environ. Sci. Technol.*, 53, 10542-10544,
764 <https://doi.org/10.1021/acs.est.9b04725>, 2019.
- 765 Benitez-Lopez, A., Alkemade, R., Schipper, A. M., Ingram, D. J., Verweij, P. A.,
766 Eikelboom, J. A. J., and Huijbregts, M. A. J.: The impact of hunting on tropical

767 mammal and bird populations, *Science*, 356, 180-183, [https://doi.org/](https://doi.org/10.1126/science.aaj1891)
768 10.1126/science.aaj1891, 2017.

769 Bracken, M. B.: Statistical methods for analysis of effects of treatment in overviews of
770 randomized trials. In: J.C. Sinclair, M.B. Bracken (Eds.) *Effective care of the*
771 *newborn infant*, Oxford University Press, 1992.

772 Chen, Z.Y., Chen, D.L., Wen, W., Zhuang, Y., Kwan, M.P., Chen, B., Zhao, B., Yang,
773 L., Gao, B.B., Li, R.Y., and Xu, B.: Evaluating the “2+26” regional strategy for air
774 quality improvement during two air pollution alerts in Beijing: Variations in PM_{2.5}
775 concentrations, source apportionment, and the relative contribution of local
776 emission and regional transport, *Atmos. Chem. Phys.*, 19, 6879-6891.
777 <https://doi.org/10.5194/acp-19-6879-2019>, 2019.

域代码已更改

778 Cheng, Y.F., Zheng, G.A., Wei, C., Mu, Q., Zheng, B., Wang, Z.B., Gao, M., Zhang, Q.,
779 He, K.B., Carmichael, G., Poschl, U., and Su, H.: Reactive nitrogen chemistry in
780 aerosol water as a source of sulfate during haze events in China, *Sci. Adv.* 2(12).
781 <https://doi.org/10.1126/sciadv.1601530>, 2016.

域代码已更改

782 China Electricity Council.: *China Power Industry Annual Development Report 2019*,
783 <https://www.cec.org.cn/yaowenkuaidi/2019-06-14/191782.html>, 2020.

域代码已更改

784 CSC (China State Council): The 11th Five-Year plan on energy saving and emissions
785 reduction, http://www.gov.cn/zhengce/content/2008-03/28/content_4877.htm,
786 2007.

域代码已更改

787 CSC (China State Council): The 12th Five-Year plan on energy saving and emissions
788 reduction. http://www.gov.cn/zwggk/2011-12/20/content_2024895.htm, 2011.

域代码已更改

789 CSC (China State Council): *Action Plan on Prevention and Control of Air Pollution*,
790 China State Council, Beijing, China. [http://www.gov.cn/zwggk/2013-](http://www.gov.cn/zwggk/2013-09/12/content_2486773.htm)
791 09/12/content_2486773.htm, 2013.

域代码已更改

792 CSC (China State Council): The 13th Five-Year plan on energy saving and emissions
793 reduction. http://www.gov.cn/zhengce/content/2016-12/05/content_5143290.htm,
794 2016.

域代码已更改

795 CSC (China State Council): Air quality targets set by the Action Plan have been fully
796 realized, http://www.gov.cn/xinwen/2018-02/01/content_5262720.htm, 2018a.

删除了: http://www.gov.cn/xinwen/2018-02/01/content_5262720.htm...

797 CSC (China State Council): Notice of the state council on issuing the three-year action
798 plan for winning the Blue Sky defense battle.
799 http://www.gov.cn/zhengce/content/2018-07/03/content_5303158.htm, 2018b.

设置了格式: 默认段落字体, 字体: 等线, 五号, 检查拼写和语法

域代码已更改

800 Dunn, O.J.: Multiple comparisons using rank sums. *Technometrics*, 6, 241-252, 1964.

801 Fountoukis, C., Racherla, P. N., Denier van der Gon, H. A. C., Polymeneas, P.,
802 Charalampidis, P. E., Pilinis, C., Wiedensohler, A., Dall'Osto, M., O'Dowd, C., and
803 Pandis, S. N.: Evaluation of a three-dimensional chemical transport model
804 (PMCAMx) in the European domain during the EUCAARI May 2008 campaign,
805 *Atmos. Chem. Phys.*, 11, 10331–10347. [https://doi.org/10.5194/acp-11-10331-](https://doi.org/10.5194/acp-11-10331-2011)
806 2011, 2011.

域代码已更改

807 Fan, C., Li, Z., Li, Y., Dong, J., van der A, R., and de Leeuw, G.: Variability of NO₂
808 concentrations over China and effect on air quality derived from satellite and
809 ground-based observations, *Atmos. Chem. Phys.*, 21, 7723-7748,
810 <https://doi.org/10.5194/acp-21-7723-2021>, 2021.

811 Gao, M., Carmichael, G. R., Wang, Y., Saide, P. E., Yu, M., Xin, J., Liu, Z., and Wang,
812 Z.: Modeling study of the 2010 regional haze event in the North China Plain, *Atmos.*
813 *Chem. Phys.*, 16, 1673–1691, <https://doi.org/10.5194/acp-16-1673-2016>, 2016.

删除了: <https://doi.org/10.5194/acp-16-1673-2016>

设置了格式: 默认段落字体, 字体: 等线, 五号

814 Geng, G., Xiao, Q., Zheng, Y., Tong, D., Zhang, Y., Zhang, X., Zhang, Q., He, K., and
815 Liu, Y.: Impact of China's air pollution prevention and control action plan on PM_{2.5}
816 chemical composition over eastern China, *Sci China Earth Sci.*, 62, 1872-1884,

删除了: .N

删除了: .Y

删除了: .X

删除了: .X

删除了: .Y

删除了: .B

826 <https://doi.org/10.1007/s11430-018-9353-x>, 2019.

827 [Geng, G., Xiao, Q., Liu, S., Liu, X., Cheng, J., Zheng, Y., Xue, T., Tong, D., Zheng,](#)
828 [B., Peng, Y., and Huang, X.: Tracking air pollution in China: Near real-time PM_{2.5}](#)
829 [retrievals from multisource data fusion, Environ. Sci. Technol., 55, 12106-12115,](#)
830 <https://doi.org/10.1021/acs.est.1c01863>, 2021.

831 [Geng, G., Zhang, Q., Tong, D., Li, M., Zheng, Y., Wang, S., and He, K.: Chemical](#)
832 [composition of ambient PM_{2.5} over China and relationship to precursor emissions](#)
833 [during 2005–2012, Atmos. Chem. Phys., 17, 9187–9203,](#)
834 <https://doi.org/10.5194/acp-17-9187-2017>, 2017.

835 Gu, B. J., Zhu, Y. M., Chang, J., Peng, C. H., Liu, D., Min, Y., Luo, W. D., Howarth, R.
836 W., and Ge, Y.: The role of technology and policy in mitigating regional nitrogen
837 pollution, Environ. Res. Lett., 6, 1, <https://doi.org/10.1088/1748-9326/6/1/014011>,
838 2011.

839 Guenther, A. B., Jiang, X., Heald, CL., Sakulyanontvittaya, T., Duhl, T., Emmons, L.
840 K., and Wang, X.: The Model of Emissions of Gases and Aerosols from Nature
841 version 2.1 (MEGAN2.1): an extended and updated framework for modeling
842 biogenic emissions, Geosci. Model Dev., 5, 1471-1492.
843 <https://doi.org/10.5194/gmd-5-1471-2012>, 2012.

844 Han, Y., Wu, Y. F., Don, H. Y., and Chen, F.: Characteristics of PM_{2.5} and its chemical
845 composition during the Asia-Pacific Economic Cooperation Summit in Beijing-
846 Tianjin-Hebei Region and surrounding cities, Environ. Sci. Technol., 40, 134-138
847 (in Chinese with English abstract), 2017.

848 Huang, R. J., Zhang, Y. L., Bozzetti, C., Ho, K. F., Cao, J. J., Han, Y. M., Daellenbach,
849 K. R., Slowik, J. G., Platt, S. M., Canonaco, F., Zotter, P., Wolf, R., Pieber, S. M.,
850 Bruns, E. A., Crippa, M., Ciarelli, G., Piazzalunga, A., Schwikowski, M.,

设置了格式: 字体颜色: 自动设置

设置了格式: 字体: (中文) TimesNewRomanPSMT

域代码已更改

851 Abbaszade, G., Schnelle-Kreis, J., Zimmermann, R., An, Z. S., Szidat, S.,
852 Baltensperger, U., El Haddad, I., and Prevot, A. S.: High secondary aerosol
853 contribution to particulate pollution during haze events in China, *Nature*, 514, 218-
854 222. <https://doi.org/10.1038/nature13774>, 2014.

855 Huang, X., Ding, A.J, Gao, J., Zheng, B., Zhou, D.R., Qi, X. M., Tang, R., Wang, J. P.,
856 Ren, C. H., Nie, W., Chi, X. G., Xu, Z., Chen, L. D., Li, Y. Y., Che, F., Pang, N. N.,
857 Wang, H. K., Tong, D., Qin, W., Cheng, W., Liu, W. J., Fu, Q. Y., Liu, B. X., Chai,
858 F. H., Davis, S. J., Zhang, Q., and He, K. B.: Enhanced secondary pollution offset
859 reduction of primary emissions during COVID-19 lockdown in China, *Natl. Sci.*
860 *Rev.*, 8, 137, <https://doi.org/10.1093/nsr/nwaa137>, 2021.

861 Ianniello, A., Spataro, F., Esposito, G., Allegrini, I., Rantica, E., Ancora, MP., Hu, M.,
862 and Zhu, T.: Occurrence of gas phase ammonia in the area of Beijing (China).
863 *Atmos. Chem. Phys.*, 10, 9487-9503, <https://doi.org/10.5194/acp-10-9487-2010>, 2010.

864 Kang, Y. N., Liu, M. X., Song, Y., Huang, X., Yao, H., Cai, X. H., Zhang, H. S., Kang,
865 L., Liu, X. J., Yan, X. Y., He, H., Zhang, Q., Shao, M., and Zhu, T.: High-resolution
866 ammonia emissions inventories in China from 1980 to 2012, *Atmos. Chem. Phys.*,
867 16, 2043-2058, <https://doi.org/10.5194/acp-16-2043-2016>, 2016.

868 Kruskal, W.H. and Wallis, W.A.: Use of ranks in one-criterion variance
869 analysis. *Journal of the American statistical Association*, 47, 583-621,
870 <https://doi.org/10.1080/01621459.1952.10483441>, 1952.

871 Kuerban, M., Waili, Y., Fan, F., Liu, Y., Qin, W., Dore, A. J., Dore, A. J., Xu, W., and
872 Zhang, F. S.: Spatio-temporal patterns of air pollution in China from 2015 to 2018
873 and implications for health risks, *Environ. Pollut.*, 258, 113659, <https://doi.org/10.1016/j.envpol.2019.113659>, 2020.

域代码已更改

删除了: <https://doi.org/10.5194/acp-10-9487-2010>

876 [Li, H., Cheng, J., Zhang, Q., Zheng, B., Zhang, Y., Zheng, G., and He, K.: Rapid](#)
877 [transition in winter aerosol composition in Beijing from 2014 to 2017: response to](#)
878 [clean air actions, Atmos. Chem. Phys., 19, 11485–11499,](#)
879 <https://doi.org/10.5194/acp-19-11485-2019>, 2019.

设置了格式: 字体颜色: 自动设置

带格式的: 缩进: 左侧: 0 厘米, 悬挂缩进: 2 字符, 首行缩进: -2 字符, 定义网格后不调整右缩进, 孤行控制, 不调整西文与中文之间的空格, 不调整中文和数字之间的空格

880 Li, H. Y., Zhang, Q., Zheng, B., Chen, C. R., Wu, N. N., Guo, H. Y., Zhang, Y. X., Zheng,
881 Y. X., Li, X., and He, K. B.: Nitrate-driven urban haze pollution during summertime
882 over the North China Plain, Atmos. Chem. Phys., 18, 5293-5306, [https://doi.org/](https://doi.org/10.5194/acp-18-5293-2018)
883 [10.5194/acp-18-5293-2018](https://doi.org/10.5194/acp-18-5293-2018), 2018.

设置了格式: 字体: (中文) TimesNewRomanPSMT, 检查拼写和语法

884 [Li, K., Jacob, D. J., Shen, L., Lu, X., De Smedt, I., and Liao, H.: Increases in surface](#)
885 [ozone pollution in China from 2013 to 2019: anthropogenic and meteorological](#)
886 [influences, Atmos. Chem. Phys., 20, 11423–11433, https://doi.org/10.5194/acp-20-](#)
887 [11423-2020](https://doi.org/10.5194/acp-20-11423-2020), 2020.

设置了格式: 字体颜色: 自动设置, 不检查拼写或语法

带格式的: 正文

888 Li, M., Liu, H., Geng, G., Geng, G. N., Hong, C. P., Liu, F., Song, Y., Tong, D., Zheng,
889 B., Cui, H. Y., Man, H. Y., Zhang, Q., and He, K. B.: Anthropogenic emission
890 inventories in China: a review, Natl. Sci. Rev., 4, 834-866.
891 <https://doi.org/10.1093/nsr/nwx150>, 2017.

892 [Li, X., Bei, N., Hu, B., Wu, J., Pan, Y., Wen, T., Liu, Z., Liu, L., Wang, R., and Li, G.:](#)
893 [Mitigating NO_x emissions does not help alleviate wintertime particulate pollution](#)
894 [in Beijing-Tianjin-Hebei, China, Environ. Pollut., 279\(X\), https://](#)
895 [10.1016/j.envpol.2021.11693](https://doi.org/10.1016/j.envpol.2021.11693), 2021.

设置了格式: 字体颜色: 自动设置

带格式的: 缩进: 左侧: 0 厘米, 悬挂缩进: 2 字符, 首行缩进: -2 字符, 定义网格后不调整右缩进, 孤行控制, 不调整西文与中文之间的空格, 不调整中文和数字之间的空格

896 Liang, F. C., Xiao, Q. Y., Huang, K. Y., Yang, X. L., Liu, F. C., Li, J. X., Lu, X. F., Liu,
897 Y., and Gu, D. F.: The 17-y spatiotemporal trend of PM_{2.5} and its mortality burden
898 in China, Proc. Natl. Acad. Sci. U. S. A., 117, 25601-25608, [https://doi.org/](https://doi.org/10.1073/pnas.1919641117)
899 [10.1073/pnas.1919641117](https://doi.org/10.1073/pnas.1919641117), 2020.

设置了格式: 字体: (中文) TimesNewRomanPSMT, 检查拼写和语法

900 Liu, J., Han, Y. Q., Tang, X., Zhu, J., and Zhu, T.: Estimating adult mortality attributable

901 to PM_{2.5} exposure in China with assimilated PM_{2.5} concentrations based on a ground
902 monitoring network, *Sci. Total. Environ.*, 568, 1253-1262, [https://doi.org/](https://doi.org/10.1016/j.scitotenv.2016.05.165)
903 10.1016/j.scitotenv.2016.05.165, 2016.

904 Liu, L., Zhang, X. Y., Wong, A. Y. H., Xu, W., Liu, X. J., Li, Y., Mi, H., Lu, X. H., Zhao,
905 L. M., Wang, Z., Wu, X. D., and Wei, J.: Estimating global surface ammonia
906 concentrations inferred from satellite retrievals, *Atmos. Chem. Phys.*, 19, 12051-
907 12066. <https://doi.org/10.5194/acp-19-12051-2019>, 2019a.

908 Liu, M. X., Huang, X., Song, Y., Tang, J., Cao, J. J., Zhang, X. Y., Zhang, Q., Wang, S.
909 X., Xu, T. T., Kang, L., Cai, X. H., Zhang, H. S., Yang, F. M., Wang, H. B., Yu, J.
910 Z., Lau, A. K. H., He, L. Y., Huang, X. F., Duan, L., Ding, A. J., Xue, L. K., Gao,
911 J., Liu, B., and Zhu, T.: Ammonia emission control in China would mitigate haze
912 pollution and nitrogen deposition, but worsen acid rain, *Proc. Natl. Acad. Sci. U. S.*
913 *A.*, 116, 7760-7765, <https://doi.org/10.1073/pnas.1814880116>, 2019b.

914 Liu, X.J., Sha, Z.P., Song, Y., Dong, H.M., Pan, Y.P., Gao, Z.L., Li, Y.E., Ma, L., Dong,
915 W.X., Hu, C.S., Wang, W.L., Wang, Y., Geng, H., Zheng, Y.H., and Gu, M.N.:
916 China's atmospheric ammonia emission characteristics, mitigation options and
917 policy recommendations, *Res. Environ. Sci.*, 34, 149-157,
918 <https://10.13198/j.issn.1001-6929.2020.11.12>, 2021.

919 Mao, S. S., Chen, T, Fu, J. M., Liang, J. L., An, X. X., Luo, X. X., Zhang, D. W., and
920 Liu, B. X.: Characteristic analysis for the thick winter air pollution accidents in
921 Beijing based on the online observations, *Journal of Safety and Environment*. 1,
922 1009-6094 (in Chinese with English abstract), 2018.

923 MEEP. The Ministry of Ecology and Environment of the People's Republic of China,
924 China Ecological Environment Bulletin.

域代码已更改

925 <http://www.mee.gov.cn/hjzl/sthjzk/zghjzkqb/>, 2019.

域代码已更改

926 Megaritis, A., Fountoukis, C., Charalampidis, P. E., Pilinis, C., and Pandis, S. N.:
927 Response of fine particulate matter concentrations to changes of emissions and
928 temperature in Europe, *Atmos. Chem. Phys.*, 13, 3423-3443,
929 <https://doi.org/10.5194/acp-13-3423-2013>, 2013.

930 MEPC. Ministry of Environment Protection of China, Ambient air quality standards
931 (GB3095-2012). <http://www.mep.gov.cn/>, 2012.

932 Morrison, H., Thompson, G., and Tatarskii, V.: Impact of cloud microphysics on the
933 development of trailing stratiform precipitation in a simulated squall line:
934 comparison of one- and two-moment schemes, *Mon. Weather. Rev.*, 137, 991-1007.
935 <https://doi.org/10.1175/2008MWR2556.1>, 2012 .

域代码已更改

936 Nakagawa, S. and Santos, E. S. A.: Methodological issues and advances in biological
937 meta-analysis, *Evol. Ecol.*, 26, 1253-1274. [https://doi.org/10.1007/s10682-012-](https://doi.org/10.1007/s10682-012-9555-5)
938 [9555-5](https://doi.org/10.1007/s10682-012-9555-5), 2012.

939 Ortiz-Montalvo, D. Häkkinen, S. A. K., Schwier, A. N., Lim, Y. B., Faye McNeill, V.,
940 and Turpin, B. J.: Ammonium addition (and aerosol pH) has a dramatic impact on
941 the volatility and yield of glyoxal secondary organic aerosol, *Environ. Sci. Technol.*,
942 48, 255-262, <https://doi.org/10.1021/es4035667>, 2014.

943 Pinder, R. W., Adams, P. J., and Pandis, S. N.: Ammonia emission controls as a cost-
944 effective strategy for reducing atmospheric particulate matter in the eastern United
945 States, *Environ. Sci. Technol.*, 41, 380-386, <https://doi.org/10.1021/es060379a>,
946 2007.

947 Ronald, J. V., Mijling, B., Ding, J. Y., Koukouli, M. E., Liu, F., Li, Q., Mao, H. Q., and
948 Theys, N.: Cleaning up the air: effectiveness of air quality policy for SO₂ and NO_x
949 emissions in China, *Atmos. Chem. Phys.*, 17, 1775-1789,

删除了: Röllin, H.B., Mathee, A., Bruce, N., Levin, J., and von Schirnding, Y. E.: Comparison of indoor air quality in electrified and un-electrified dwellings in rural South African villages. *Indoor Air*, 14, 208-16. <https://doi.org/10.1111/j.1600-0668.2004.00238.x>, 2004.

955 <https://doi.org/10.5194/acp-17-1775-2017>, 2017.

956 Shang, Z.Y., Zhou, F., Smith, P., Saikawa, E., Ciais, P., Chang, J.F., Tian, H.Q., Del
957 Grosso, S.L., Ito, A., Chen, M.P., Wang, Q.H., Bo, Y., Cui, X.Q., Castaldi, S.,
958 Juszczak, P., Kasimire, A., Magliulo, V., Medinets, S., Medinets, V., Rees, R. M.,
959 Wohlfahrt, G., and Sabbatini, S: Weakened growth of cropland-N₂O emissions in
960 China associated with nationwide policy interventions, *Glob. Change. Biol.*, 25,
961 3706-3719, <https://doi.org/10.1111/gcb.14741>, 2021.

962 Sun, Y. L., Zhuang, G. S., Tang, A. H., Wang, Y., and An, Z. S.: Chemical characteristics
963 of PM_{2.5} and PM₁₀ in haze-fog episodes in Beijing, *Environ. Sci. Technol.*, 40, 3148-
964 3155, <https://doi.org/10.1021/es051533g>, 2006.

965 Tao, J., Gao, J., Zhang, L. M., Wang, H., Qiu, X. H., Zhang, Z. S., Wu, Y. F., Chai, F.
966 H., and Wang, S. L: Chemical and optical characteristics of atmospheric aerosols in
967 Beijing during the Asia-Pacific Economic Cooperation China 2014, *Atmos.*
968 *Environ.*, 144, 8-16, <https://doi.org/10.1016/j.atmosenv.2016.08.067>, 2016.

969 Wang S.: How to promote ultra-low emissions during the 14th Five-Year Plan? *China.*
970 *Environment. News.* http://epaper.cenews.com.cn/html/2021-04/30/node_7.htm,
971 2021a.

972 Wang, G. H., Zhang, R. Y., Gomez, M. E., Yang, L. X., Zamora, M. L., Hu, M., Lin, Y.,
973 Peng, J. F., Guo, S., Meng, J. J., Li, J. J., Cheng, C. L., Hu, T. F., Ren, Y. Q., Wang,
974 Y. S., Gao, J., Cao, J. J., An, Z. S., Zhou, W. J., Li, G. H., Wang, J. Y., Tian, P. F.,
975 Marrero-Ortiz, W., Secrest, J., Du, Z. F., Zheng, J., Shang, D. J., Zeng, L. M., Shao,
976 M., Wang, W. G., Huang, Y., Wang, Y., Zhu, Y. J., Li, Y. X., Hu, J. X., Pan, B., Cai,
977 L., Cheng, Y. T., Ji, Y. M., Zhang, F., Rosenfeld, D., Liss, P. S., Duce, R. A., Kolb,
978 C. E., and Molina, M. J.: Persistent sulfate formation from London Fog to Chinese
979 haze, *Proc. Natl. Acad. Sci. U. S. A.*, 113, 13630-13635, <https://doi.org/>

删除了: Sulaymon, I.D., Zhang, Y., Hopke, P. K., Zhang, Y., Hua, J., and Mei, X.: COVID-19 pandemic in Wuhan: Ambient air quality and the relationships between criteria air pollutants and meteorological variables before, during, and after lockdown, *Atmos Res.*, 250. <https://doi.org/10.1016/j.atmosres.2020.105362>, 2021.

域代码已更改

986 10.1073/pnas.1616540113, 2016.

987 Wang, L., Chen, X., Zhang, Y., Li, M., Li, P., Jiang, L., Xia, Y., Li, Z., Li, J., Wang, L.,
988 Hou, T., Liu, W., Rosenfeld, D., Zhu, T., Zhang, Y., Chen, J., Wang, S., Huang, Y.,
989 Seinfeld, J. H., and Yu, S.: Switching to electric vehicles can lead to significant
990 reductions of PM_{2.5} and NO₂ across China, *One Earth*, 4, 1037–1048,
991 <https://doi.org/10.1016/j.oneear.2021.06.008>, 2021b.

992 Wang, L., Yu, S., Li, P., Chen, X., Li, Z., Zhang, Y., Li, M., Mehmood, K., Liu, W., Chai,
993 T., Zhu, Y., Rosenfeld, D., and Seinfeld, J. H.: Significant wintertime PM_{2.5}
994 mitigation in the Yangtze River Delta, China, from 2016 to 2019: observational
995 constraints on anthropogenic emission controls, *Atmos. Chem. Phys.*, 2, 14787–
996 14800, <https://doi.org/10.5194/acp-20-14787-2020>, 2020a.

997 Wang, Q.H., Zhou, F., Shang, Z.Y., Ciais, P., Winiwarter, W., Jackson, R. B., Tubiello,
998 F.N., Janssens-Maenhout, G., Tian, H. Q., Cui, X. Q., Canadell, J.G., Piao, S. L.,
999 and Tao, S.: Data-driven estimates of global nitrous oxide emissions from cropland,
1000 *Natl. Sci. Rev.*, 7, 441-452, <https://doi.org/10.1093/nsr/nwz087>, 2020b.

1001 Wang, S. X, Xing, J., Jang, C., Jang, C. R., Zhu, Y., Fu, J. S., and Hao, J. M.: Impact
1002 assessment of ammonia emissions on inorganic aerosols in East China using
1003 response surface modeling technique, *Environ. Sci. Technol.*, 45, 9293-9300,
1004 <https://doi.org/10.1021/es2022347>, 2011.

1005 Wang, Y. H., Wang, Y. S., Wang, L.L., Petaja, T., Zha, Q.Z., Gong, C.S., Li, S.X., Pan,
1006 Y. P., Hu, B., Xin, J. Y., and Kulmala, M.: Increased inorganic aerosol fraction
1007 contributes to air pollution and haze in China, *Atmos. Chem. Phys.*, 19, 5881-5888.
1008 <https://10.5194/acp-19-5881-2019>, 2019a.

1009 Wang, Y., Zhang, Q. Q., He, K.B., Zhang, Q., and Chai, L.: Sulfate-nitrate-ammonium
1010 aerosols over China: Response to 2000-2015 emission changes of sulfur dioxide,

域代码已更改

域代码已更改

域代码已更改

- 1011 nitrogen oxides, and ammonia, *Atmos. Chem. Phys.*, **13**, 2635–2652.
1012 <https://doi.org/10.5194/acp-13-2635-2013>, 2013.
- 1013 Wang, Y.C., Chen, J., Wang, Q.Y., Qin, Q.D., Ye, J.H., Han, Y.M., Li, L., Zhen, W., Zhi,
1014 Q., Zhang, Y.X., and Cao, J.J.: Increased secondary aerosol contribution and
1015 possible processing on polluted winter days in China, *Environ. Int.*, **127**.
1016 <https://doi.org/10.1016/j.envint.2019.03.021>, 2019b.
- 1017 Wei, J., Li, Z. Q., Cribb, M., Huang, W., Xue, W.H., Sun, L., Guo, J. P., Peng, Y. R., Li,
1018 J., and Lyapustin, A.: Improved 1 km resolution PM_{2.5} estimates across China using
1019 enhanced space–time extremely randomized trees, *Atmos. Chem. Phys.*, **20**, 3273–
1020 3289. <https://doi.org/10.5194/acp-20-3273-2020>, 2020.
- 1021 Wei, J., Li, Z. Q., Lyapustin, A., Sun, L., Peng, Y. R., Xue, W. H., Su, T. N., and Cribb,
1022 M.: Reconstructing 1-km-resolution high-quality PM_{2.5} data records from 2000 to
1023 2018 in China: spatiotemporal variations and policy implications, *Remote. Sens.*
1024 *Environ.*, **252**, 112136, <https://doi.org/10.1016/j.rse.2020.112136>, 2021.
- 1025 Wu, Y. J., Wang, P., Yu, S. C., Wang, L. Q., Li, P. F., Li, Z., Mehmood, K., Liu, W. P.,
1026 Wu, J., Lichtfouse, E., Rosenfeld, D., and Seinfeld, J. H.: Residential emissions
1027 predicted as a major source of fine particulate matter in winter over the Yangtze
1028 River Delta, China, *Environ. Chem. Lett.*, **16**, 1117–1127.
1029 <https://doi.org/10.1007/s10311-018-0735-6>, 2018a.
- 1030 Wu, Y. Y., Xi, X. C., Tang, X., Luo, D. M., Gu, B. J., Lam, S. K., Vitousek, P. M., and
1031 Chen, D. L.: Policy distortions, farm size, and the overuse of agricultural chemicals
1032 in China, *Proc. Natl. Acad. Sci. U. S. A.*, **115**, 7010–7015.
1033 <https://doi.org/10.1073/pnas.1806645115>, 2018b.
- 1034 Xiao, Q.Y, Geng, G.N., Liang, F.C., Wang, X., Lv, Z., Lei, Y., Huang, X.M., Zhang, Q.,
1035 Liu, Y., and He, K.B: Changes in spatial patterns of PM_{2.5} pollution in China 2000–

1036 2018: Impact of clean air policies, *Environ. Int.*, 141, 105776, [https://doi.org/](https://doi.org/10.1016/j.envint.2020.105776)
1037 10.1016/j.envint.2020.105776, 2020.

1038 Xiao, Q.Y., Zheng, Y.X., Geng, G.N., Chen, C.H., Huang, X.M., Che, H.Z., Zhang, X.Y.,
1039 He, K.B., and Zhang, Q.: Separating emission and meteorological contribution to
1040 PM_{2.5} trends over East China during 2000–2018, *Atmos. Chem. Phys.*, 21, 9475-
1041 9496, <https://doi.org/10.5194/acp-21-9475-2021>, 2021.

1042 Xing, J., Liu, X., Wang, S. X., Wang, T., Ding, D., Yu, S., Shindell, D., Ou, Y .,
1043 Morawska, L., Li, S. W., Ren, L., Zhang, Y. Q., Loughlin, D., Zheng, H. T., Zhao,
1044 B., Liu, S. C., Smith, K. R., and Hao, J. M.: The quest for improved air quality may
1045 push China to continue its CO₂ reduction beyond the Paris Commitment, *Proc. Natl.*
1046 *Acad. Sci. U. S. A.*, 117, 29535-29542, <https://doi.org/10.1073/pnas.2013297117>,
1047 2021.

1048 Xu, Q. C., Wang, S. X., Jiang, J. K., Bhattarai, N., Li, X. X., Chang, X., Qiu, X. H.,
1049 Zheng, M., Hua, Y., and Hao, J. M.: Nitrate dominates the chemical composition of
1050 PM_{2.5} during haze event in Beijing, China, *Sci. Total. Environ.*, 689, 1293-1303,
1051 <https://doi.org/10.1016/j.scitotenv.2019.06.294>, 2019.

1052 Xu, W., Song, W., Zhang, Y. Y., Liu, X. J., Zhang, L., Zhao, Y. H., Liu, D. Y., Tang, A.
1053 H., Yang, D. W., Wang, D. D., Wen, Z., Pan, Y. P., Fowler, D., Collett, J. L., Erisman,
1054 J. W., Goulding, K., Li, Y., and Zhang, F. S.: Air quality improvement in a megacity:
1055 implications from 2015 Beijing Parade Blue pollution control actions, *Atmos.*
1056 *Chem. Phys.*, 17, 31-46. <https://doi.org/10.5194/acp-17-31-2017>, 2017.

1057 Xu, W., Wu, Q.H., Liu, X.J., Tang, A.H., Dore, A.J., and Heal, M.R.: Characteristics of
1058 ammonia, acid gases, and PM_{2.5} for three typical land-use types in the North China
1059 Plain, *Environ Sci Pollut R.*, 23, 1158-1172. [https://doi.org/10.1007/s11356-015-](https://doi.org/10.1007/s11356-015-5648-3)
1060 5648-3, 2016.

域代码已更改

1061 Xue, T., Liu, J., Zhang, Q., Geng, G.N., Zheng, Y.X., Tong, D., Liu, Z., Guan, D.B., Bo,
1062 Y., Zhu, T., He, K.B., and Hao, J.M.: Rapid improvement of PM_{2.5} pollution and
1063 associated health benefits in China during 2013–2017, *Sci. China Earth Sci.*, 62,
1064 1847-1856, <https://doi.org/10.1007/s11430-018-9348-2>, 2019.

1065 Yang, F., Tan, J., Zhao, Q., Du, Z., He, K., Ma, Y., Duan, F., Chen, G., and Zhao, Q.:
1066 Characteristics of PM_{2.5} speciation in representative megacities and across China.
1067 *Atmos. Chem. Phys.*, 11, 5207-5219, <https://doi.org/10.5194/acp-11-5207-2011>,
1068 2011.

域代码已更改

1069 Ying, H., Yin, Y. L., Zheng, H. F., Wang, Y. C., Zhang, Q. S., Xue, Y. F., Stefanovski,
1070 D., Cui, Z. L., and Dou, Z. X.: Newer and select maize, wheat, and rice varieties
1071 can help mitigate N footprint while producing more grain, *Glob. Change. Biol.*, 12,
1072 4273-4281, <https://doi.org/10.1111/gcb.14798>, 2019.

1073 Yu, S.C., Dennis, R., Roselle, S., Nenes, A., Walker, J., Eder, B., Schere, K., Swall, J.,
1074 and Robarge, W.: An assessment of the ability of three-dimensional air quality
1075 models with current thermodynamic equilibrium models to predict aerosol NO₃⁻, *J*
1076 *Geophys Res-Atmos.*, 110(D7). <https://doi.org/10.1029/2004JD004718>, 2005.

域代码已更改

1077 Yue, H. B., He, C. Y., Huang, Q. X., Yin, D., and Bryan, B. A.: Stronger policy required
1078 to substantially reduce deaths from PM_{2.5} pollution in China, *Nat. Commun.*, 11,
1079 1462, <https://doi.org/10.1038/s41467-020-15319-4>, 2020.

1080 [Zhai, S., Jacob, D.J., Wang, X., Liu, Z., Wen, T., Shah, V., Li, K., Moch, J.M., Bates,
1081 K.H., Song, S. and Shen, L.: Control of particulate nitrate air pollution in China, *Nat.*
1082 *Geosci.*, 14, 389-395. <https://doi.org/10.1038/s41561-021-00726-z>, 2021.](#)

设置了格式: 字体颜色: 自动设置, 不检查拼写或语法
带格式的: 正文

1083 Zhan, X.Y., Adalibieke, W., Cui, X.Q., Winiwarter, W., Reis, S., Zhang, L., Bai, Z.H.,
1084 Wang, Q.H., Huang, W.C., and Zhou, F.: Improved estimates of ammonia emissions
1085 from global croplands, *Environ. Sci. Technol.*, 55, 1329-1338,

域代码已更改

域代码已更改

域代码已更改

1086 <https://doi.org/10.1021/acs.est.0c05149>, 2021.

域代码已更改

1087 Zhang, L., Jacob, D. J., Knipping, E. M., Kumar, N., Munger, J. W., Carouge, C. C.,
1088 van Donkelaar, A., Wang, Y. X., and Chen, D: Nitrogen deposition to the United
1089 States: distribution, sources, and processes, *Atmos. Chem. Phys.*, 12, 4539–4554,
1090 <https://doi.org/10.5194/acp-12-4539-2012>, 2012.

域代码已更改

1091 Zhang, Q., Zheng, Y. X., Tong, D., Shao, M., Wang, S. X., Zhang, Y. H., Xu, X. D.,
1092 Wang, J. N., He, H., Liu, W. Q., Ding, Y. H., Lei, Y., Li, J. H., Wang, Z. F., Zhang,
1093 X. Y., Wang, Y. S., Cheng, J., Liu, Y., Shi, Q. R., Yan, L., Geng, G. N., Hong, C. P.,
1094 Li, M., Liu, F., Zheng, B., Cao, J. J., Ding, A. J., Gao, J., Fu, Q. Y., Huo, J. T., Liu,
1095 B. X., Liu, Z. R., Yang, F. M., He, K. B., and Hao, J. M.: Drivers of improved PM_{2.5}
1096 air quality in China from 2013 to 2017, *Proc. Natl. Acad. Sci. U. S. A.*, 49, 24463-
1097 24469, <https://doi.org/10.1073/pnas.1907956116>, 2019.

域代码已更改

1098 Zhang, X. M., Gu, B. J., van Grinsven, H., Lam, S.K., Liang, X., Bai, M., and Chen,
1099 D.L.: Societal benefits of halving agricultural ammonia emissions in China far
1100 exceed the abatement costs. *Nat. Commun.*, 11, 4357,
1101 <https://doi.org/10.1038/s41467-020-18196-z>, 2020a.

域代码已更改

设置了格式: 字体颜色: 自动设置

1102 [Zhang, Y., Vu, T. V., Sun, J., He, J., Shen, X., Lin, W., Zhang, X., Zhang, J., Gao, W.,](#)
1103 [Wang, Y., Fu, T., Ma, Y., Li, W., and Shi, Z.: Significant changes in chemistry of](#)
1104 [fine particles in wintertime Beijing from 2007 to 2017: Impact of clean air actions,](#)
1105 [Environ. Sci. Technol.](#), 54, 1344-1352, <https://doi.org/10.1021/acs.est.9b04678>,
1106 [2020b](#),

带格式的: 正文, 缩进: 左侧: 0 厘米, 悬挂缩进: 2 字符, 首行缩进: -2 字符, 定义网格后不调整右缩进, 不调整西文与中文之间的空格, 不调整中文和数字之间的空格, 到齐到网格

设置了格式: 默认段落字体, 字体: (默认) 等线, (中文) 等线, 五号

1107 Zhang, Y., Chen, X., Yu, S., Wang, L., Li, Z., Li, M., Liu, W., Li, P., Rosenfeld, D., and
1108 Seinfeld, J. H: City-level air quality improvement in the Beijing-Tianjin-Hebei
1109 region from 2016/17 to 2017/18 heating seasons: Attributions and process analysis,

设置了格式: 字体: (中文) TimesNewRomanPSMT

1110 Environ. Pollut., 274, <https://doi.org/10.1016/j.envpol.2021.116523>, 2021a.

域代码已更改

1111 Zhang, Y., Liu, X., Zhang, L., Tang, A., Goulding, K., and Collett Jr, J.L.: Evolution of
1112 secondary inorganic aerosols amidst improving PM_{2.5} air quality in the North China

删除了: .Y

删除了: .J

删除了: .H

1113 Plain, Environ. Pollut., 281, 117027,

域代码已更改

1114 <https://doi.org/10.1016/j.envpol.2021.117027>, 2021b.

1115 Zheng, B., Tong, D., Li, M., Hong, C. P., Geng, G. N., Li, H. Y., Li, X., Peng, L. Q.,

1116 Qi, J., Yan, L., Zhang, Y. X., Zhao, H. Y., Zheng, Y. X., He, K. B., and Zhang, Q.:

1117 Trends in China's anthropogenic emissions since 2010 as the consequence of clean

1118 air actions, Atmos. Chem. Phys., 18, 14095-14111, [https://doi.org/10.5194/acp-18-](https://doi.org/10.5194/acp-18-14095-2018)

域代码已更改

1119 14095-2018, 2018.

1120 [Zheng, G. J., Duan, F. K., Su, H., Ma, Y. L., Cheng, Y., Zheng, B., Zhang, Q., Huang,](#)

设置了格式: 字体颜色: 自动设置

1121 [T., Kimoto, T., Chang, D., Pöschl, U., Cheng, Y. F., and He, K. B.: Exploring the](#)

1122 [severe winter haze in Beijing: the impact of synoptic weather, regional transport](#)

1123 [and heterogeneous reactions, Atmos. Chem. Phys., 15, 2969–2983,](#)

1124 <https://doi.org/10.5194/acp-15-2969-2015>, 2015.

1125

1126 设置了格式: 字体颜色: 自动设置

1127